POLITECNICO DI TORINO

College of Engineering for the Environment and the Territory

Master's Degree Course in

PETROLEUM AND MINING ENGINEERING

ANALYSIS AND MANAGEMENT OF THE DRILLING ACTIVITY

DRILL CUTTINGS RE-INJECTION: FRACTURING PROCESS AND SLURRY COMPOSITION OPTIMIZATION

SUPERVISOR: PROF. RAFFAELE ROMAGNOLI

THESIS BY: JOANNE DIB

INDEX

Table of figures

ABSTRACT

The upstream activities of oil and gas industry for future energy demand are increasing year after year; this increase will be associated with more waste generation; thus, an intensification of environmental legislations will be expected to prevent the negative impact of the different types of waste, primarily used drilling fluids and drill cuttings especially oil contaminated ones, on the environment. As the world today is heading towards more sustainable and environmental approaches to reduce the contribution to the global warming caused by the industrial activity; and as the methane and carbon dioxide, which are the main gases contributing to the global warming and are mainly produced by agriculture, oil and gas, mining, and waste management industries; all industrial firms are forced to respect all the policies imposed by the organizations defending the environment

As a result, many companies have voluntarily adopted waste management options with more benign environmental impacts. Drill Cuttings Re-Injection (DCRI) is a process developed as an environmentally friendly and zero discharge technology in upstream oil and gas industry. It has been recognized to be cost-effective and the best solution to manage drilling waste in remote and environmentally sensitive areas, including jungles, the Arctic, and offshore fields, where traditional disposal techniques are not viable.

The process of drill cuttings re-injection is a means to dispose of accumulated oilfield wastes by deep well injection.

This work describes the mechanism by which the fracture propagates after the injection of the slurry and the

I. INTRODUCTION

Wastes generated during drilling in the oil and gas industry should be safely disposed of in a manner to avoid any contamination to the environment. Implementing a waste management system to support operations allows planning for the reduction of waste streams generated by reusing or recycling some material and the use of different options for treatment or disposal of the waste either at surface or into subsurface. Different methods are employed onshore and offshore to manage drilling wastes, depending on what state and federal regulations allow and how costly those options are for the wells in question. Offshore, the options are limited to discharge, underground injection, and transport back to shore disposal; whereas, onshore there is a wider range of options: some wastes are managed onsite while others are removed to offsite commercial disposal facilities. The onshore waste management options employed include landspreading and landfarming, evaporation and burial onsite, underground injection, incineration and other thermal treatment, bioremediation and composting, and reuse and recycling.

The major cost for drilled cuttings disposal is handling and disposition, in addition to shipment to onshore locations, plus the cost to clean and move the drill cuttings several times to comply with ever tightening environmental regulations. The Cuttings re-injection process is an option that handles drill cuttings waste only once. It is considered as an on-site disposal method that fully comply with zero discharge to the environment in addition of being inexpensive relative to many environmental solutions which are not permanent. The cuttings re-injection process has been given various names including: Slurry Fracture Injection, Fracture Slurry Injection, Drill Cuttings Injection, Grind and Inject.

Cuttings Re-Injection is a process used by the petroleum industry to dispose the accumulated oilfield wastes by deep well injection. The process yields considerable advantages to the operator over conventional disposal methods. The CRI provides an environmentally attractive and permanent disposal solution for considerable volumes of non-hazardous oilfield wastes, and has minimal impact on surface land use. Also, it reduces the long-term liability to the operator while reducing transportation and disposal costs. This process consists of grinding the

solid waste to a relatively fine consistency, mixing the cutting with water and/or other liquids (often seawater, collected stormwater, other fresh water, used drilling muds, or produced water, as approved by the regulatory agency) to form a slurry, and disposing of the slurry by pumping it down a vertical well at a high enough pressure to create fractures within the target formation. The injected slurry is then emplaced in the fractures created by the force of the injection. Some other potential solid waste can be also disposed using this technique like Naturally Occurring Radioactive Materials (NORM) that are present in produced water, scale, and sand from oilfields in many regions such as the Gulf Coast of the U.S. in Addition, some toxic solid wastes could be permanently disposed under the right geologic conditions. This will be possible because deep disposal carries such minimal environmental risk and the isolation will be complete.

II. CUTTINGS RE-INJECTION

1. General description

Due to the strict environmental regulations, Cuttings Re-Injections technique has been more and more developed as it is considered as an environmentally sound, cost-effective method of zero discharge or total containment waste disposal. Since some drilling waste management practices used in the past are harmful for the environment and public health, some companies voluntarily adopted waste management options that have less environmental impacts. In offshore drilling, the transportation of the waste onshore can be costly (especially if it is transported for long distances) and represent accidental risk of fluid leakages or gaseous emissions; or the waste can be directly discharged in the sea but only for aqueous-based cuttings as they require little or no treatment before disposal. But recent strict regulations do not allow dumping of contaminated waste directly into the sea; in this case, cuttings re-injection is the most suitable waste disposal technique to use. Environmental regulations are based upon cradle-to-grave concept; thus, the operator never relinquishes responsibility for the drill cuttings and the chemicals left on them.

Different types of waste streams are produced during oil and gas exploration and production operations. These streams include produced water, drilling wastes: cuttings, drilling mud, completion and workover fluids; as well as wastewaters, including technical waters from facilities, rain waters, grey waters, washing waters, etc. The mud used in the drilling activity is classified based on its fluid phase alkalinity, dispersion, and the type of chemical used in its formulation; They are classified as water-based (WBM), oil-based (OBM) or synthetic (SBM). This drilling fluid have many properties, such as cooling and lubricating the drill bit, cleaning the hole bottom, carrying cuttings to the surface, controlling formation pressures, and improving the function of the drill string and tools in the hole… In this technology, the cuttings carried by the mud are circulated through vibrating screens called shale shakers to be separated from the mud. The separated mud is

treated to be re-used, whereas the drill cuttings to be injected are then mixed with water that degrades the particles into an acceptable size. The slurry is injected through a well using pumps into selected formations.

Oil and gas wells are constructed with multiple layers of pipes called casing. A well is drilled from top to bottom in a series of segments not at the same diameter. The top segment is drilled starting at the surface and has the largest diameter hole. After a certain depth (usually between 30-50 m and at maximum around 100 m), the hole is lined with casing that is slightly smaller than the diameter of the hole, and cement is pumped into the space between the wall of the drilled hole and the outside of the casing. Next, a smaller diameter hole is drilled to a lower depth, and another casing string is installed to that depth and cemented. This process may be repeated several more times. The final number of casing strings depends on the total depth of the well and the sensitivity of the formations through which the well passes.

There exist two common forms of slurry injection which are annular injection and tubular injection through abandoned wells or into disposal well (Fig 1). An injection well can be intentionally drilled for drilling waste injection purposes (dedicated wells) or be refitted from its original purpose (converted or redundant wells). Annular injection introduces the waste slurry through the space between two casing strings. At the lower end of the outermost casing string, the slurry enters the formation. The tubular injection alternative involves injection through a dedicated disposal well, completed with tubing and packer giving access to either an open hole or a perforated casing interval at the depth of an injection formation. The casing must be cemented below, through, and above the proposed injection zone to ensure the waste is confined to the intended receiving zone. The allowable injection pressures for annulus injectors are often lower than the allowable pressures for dedicated wells because of casing burst and collapse limitations for annulus injectors. Many annular injection jobs are designed to receive wastes from just one well. On multiwell platforms or onshore well pads, for each successive well, the drilling wastes are injected into previously drilled wells. In this mode, no single injection well is used for more than a few weeks or months. Other injection programs, particularly those with dedicated disposal well, may inject into the same well for months [7].

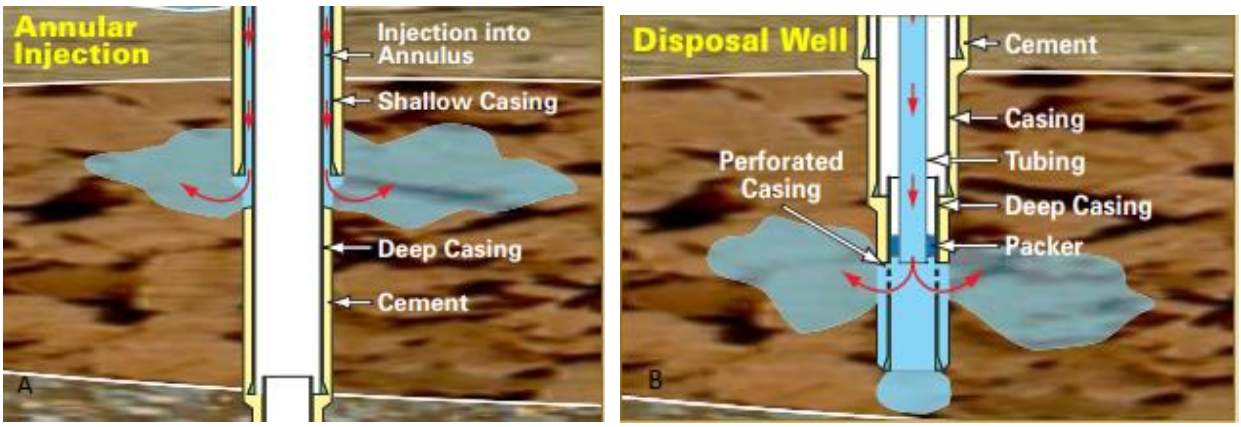

Fig 1. Waste injection into: A) annular space, B) disposal well

2. History

The first drill cuttings in the form of waste slurry underground injection projects started with the injection of small volumes of waste in the annular or tubular wellbore at an offshore drilling project in an environmentally sensitive area. These injection wells were located in the Gulf of Mexico, and it began in the mid-1980s. After the success of this project, similar new projects were carried out in the Gulf of Mexico (Ewing Bank and Fushon); the North Sea (Vallhal, Ekofisk, Ula, Gyda and Clyde); the North Slope in Alaska (Prudhoe and Endicott); Canada (Panuke); Venezuela (Pedernalis); Russian Federation (Sakhalin Islands and Western Siberia); Western Canada and other areas where weather conditions, strict regulations and logistics problems made this method a viable disposal option. During the 1990s, cuttings re-injection became a proven method as an environmentally safe and economically viable solution for the disposal of cuttings from oil and gas exploration and production activities into subsurface formations. Some oil and gas exploration and production companies like Conoco Inc. in the early 1990s successfully tried out an annular injection of slurry waste composed of waste wash water, oil-coated drilling cuttings and nonhazardous additional waste generated on drilling rigs, such as glass, paper, pallets, plastics, etc. By the end of 2001, in terms of disposal volumes for drilling waste, Alaska has injected the largest volumes (10 to $14*10^6$ barrels) in one well, followed by Canada. The North Sea has several projects that have injected between 0.25 and $2*10^6$ barrels of waste in each well.

Although subsurface injections of waste materials from drilling activities is a well-known and successful technology whose effectiveness has been confirmed through time, there are many challenges, such as frequent changes in regulation, selection of suitable geological formation, monitoring and verification of injection process, design of the whole process, etc.

According from one of the leading companies in cuttings re-injection technology (Bruno et al. from Terralog Technologies), there are three main engineering goals in the waste injection project:

- To secure injected waste containment within the desired formation (environmental management).
- To maintain maximum injectivity during the implementation of the project with minimum well workover intervention (cost management).
- To maximize formation storage capacity and well life (asset management) [8] .

3. Process and equipment used

Implementation of a drill cuttings re-injection operation involves identification, collection and transportation of solid waste from control equipment on the rig to a slurrification unit. In this technology, the cuttings should be separated from the drilling mud. The mixture of cuttings and mud is circulated through vibrating screens called shale shakers. After the liquid mud has passed through the screens, it is used for recirculation through the drill pipes, the separated rocks remaining on top of the shale shaker screen. These cuttings are directed down the screen using a vibration action. For better performance, or to completely separate cuttings from mud, several shale shakers are used. For example, first, second, and third shale shakers are known as primary, secondary, and tertiary shakers. The primary shakers use coarse screens to remove the larger cuttings. The secondary shakers use fine mesh screens to remove much smaller particles, and tertiary shakers are used to separate very fine particles. Generally, primary and secondary sale shakers are used. Using more shakers might create problems: for example, strong vibration of shakers can break up the cuttings into comparatively much smaller particles, which can in turn become very difficult to remove from mud.[5] The cuttings are further treated with drying shakers using high gravitational separation, vertical or horizontal rotary cuttings dryers, screw-type squeeze

presses, or centrifuges. The ground cuttings are then mixed with water (usually seawater) that degrades the particles into an acceptable size, ranging from 2 to 350 microns to form a slurry which rheological properties should be adjusted to maintain the continuous injectivity throughout the operation. Small particle sizes are necessary to prevent bridging and plugging of either the re-injection annulus or disposal fracture in the near-well region; also, solid wastes should not be reduced in size to finer grain because they tend to clog the pore space in the disposal formation. Slurry properties depend upon the lithology of the drilled section, particle size distribution and the mixing ratio of cuttings with seawater. The solid concentration in the slurry can be as high as 30 to 40 percent by volume for fine grained material (<150 μm) and on the order of 20 percent by volume for coarser materials.[14] The waste slurry is prepared to be pumped into sub-surface fractures under high pressure into the disposal formation. When the slurry is ready for injection, the underground formation is prepared to receive it. First, clear water is rapidly injected to pressurize the system and initiate fracturing of the formation. When the water starts flowing freely at the fracture pressure, the slurry is introduced into the well. The waste slurry can be injected as a single continuous process or as a series of smaller-volume intermittent cycles. Offshore, where drilling is continuous and storage space is not adequate to operate in a daily batch manner, continuous injection must take place as new wells are being drilled. In these cases, the operators should carefully monitor the pressure to be aware of the changes occurring in formation injectivity, and to identify incipient problems. Most of other injection jobs are designed to inject intermittently (batch process). This process consists of injecting roughly the same volumes of slurry and shutting-in the well after each injection. Periodic injection stages last generally for 8 to 14 hours; whereas, shut-in periods last from 10 to 72 hours. This allows the disposal fracture to close onto the cuttings and to dissipate any build-up of pressure in the disposal formation. This fracture closure and local fracture closure pressure increase due to solids promote new fracture creation from next batch injection. Each batch injection depends upon the batch volume and injection rate. At the end of the batch injection, additional water is injected to flush solids from the wellbore, then pumping stops. The pressure in the formation will decline as the liquid portion of the slurry bleeds off over the next few hours, and the solids will be trapped in place in the formation. The frequency of the intermittent injection cycles depends on the rate of drilling waste generation. By injecting intermittently, new fractures are induced each day rather than lengthening the original fracture; this minimizes

the probability that the fracture extends outside the target formation and it also allows the storage of a larger volume of solid material inside the fracture. [9]

The type of surface equipment required to process the drilled cuttings is based on a number of parameters established after dressing down-hole considerations. The properties of the drill cuttings dictate the type of grinding equipment required. In zero-discharge operations, the rig cannot drill if the CRI surface equipment is not adequately designed and installed to stay ahead of the drill rate/surge conditions. The cost for CRI equipment/related costs skyrockets when the drilling progress is negatively impacted.[6] Fig.2 is a representation of the cutting re-injection unit. It consists of a feed hopper, conveyance system, grinding and mixing system, water supply pump, high pressure injection pumps and storage tanks for solids, liquid waste and water. All elements are placed onsite within approximately 60 m from the wellhead of the injection well. The first part of the system consists of the drilling cuttings transportation system used for waste transportation from sources up to the slurrification unit. In the case of drilling cuttings, the simplest way for their transportation from shakers to the slurrification unit is by gravity, but there are also several other methods like auger or belt conveyors, vacuum transport systems or pneumatic bulk transports and storage systems. The appropriate waste transportation system depends on the drilling rig configuration and arrangement of equipment on it, and its efficiency depends on the quantity and composition of the waste, distance and elevation from waste sources to the slurrification unit, time interval from generation of the waste and slurry preparation and injection, etc. the slurrification unit is the second part of the slurry preparation and disposal unit, and it consists of a coarse tank (for mixing and blending of waste with water by specially designed centrifugal pumps); a classification shaker and grinder (for separation of particles based on their size and additional grinding of particles that are too large) and a fines tank (for final conditioning of the slurry by adding additional water and additives (corrosion inhibitors, biocide and friction reducers) in order to assure the desired slurry properties and quality control). The third part of the slurry preparation and disposal unit is an injection system consisting of a holding tank (for monitoring of the injection process. Although the slurry waste is traditionally injected by a positive displacement plunger or piston/liner-type triplex mud pumps, new laboratory research and field trials conducted indicate that multistage centrifugal pumps could be advantageous in some situations. In some situations, as in the case of oil and gas exploration and production waste injection

in polar regions, it is necessary to heat up the waste slurry preparation water because of frozen waste material in the reservoir pit or to apply winterized measures for the entire unit to assure a minimal internal temperature of 17^0C. [8]

In order to conduct this process, some data are required. These data and their description are given in the table 1 below:[13]

Required data	**Description**
Injection batch volumes and injection rates	Injection of the slurry is often conducted intermittently in batches into the selected disposal formation, followed by a period of shut-in. depending upon the batch volume and the injection rate, each batch injection may last from less than an hour to several days or even longer.
Minimum in situ stress	Most important in fracture simulation that controls fracture height growth, fracture azimuth and vertical and horizontal orientation, fracture width, treatment pressures, fracture conductivity, and wastes containment in disposal horizon.
Pore pressure	Very critical parameter to planning and carrying out successful CRI, because the stress state of the poroelastic medium is directly influenced by pore pressure or reservoir pressure.
Young's modulus	It is the ratio of longitudinal stress to longitudinal strain, which has significant effect on fracture geometry, especially on fracture width.
Poisson's ratio	It is a measure of the compressibility of material perpendicular to applied stress that has significant effect on fracture geometry.
Casing setting depths and injection point	The target which the slurry has to be injected via annulus or dedicated well
Fluid leak-off data	Means the leaking of fluid from the surface of a fracture into the surrounding rock formation. It's an important parameter controlling the size and geometry of hydraulically induced fracture.
Slurry rheology	The study of deformation and flow of matter, that crucial for maintaining zonal isolation.
Fracture toughness	It is an important parameter in fracture modelling and is a measure of a material's resistance to fracture propagation.

Table 1: Data required to conducte the CRI process

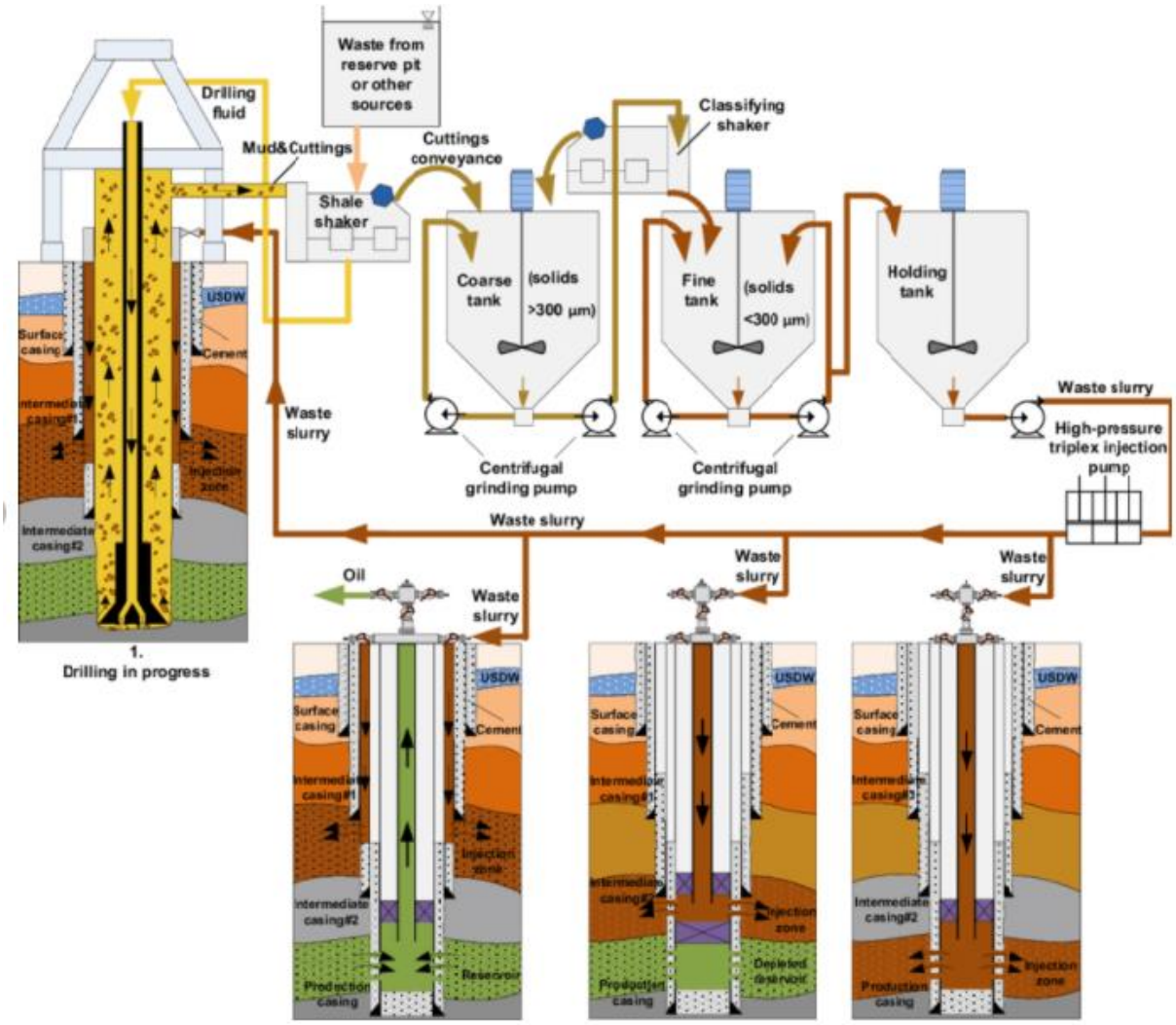

Fig.2: Waste slurry preparation and disposal unit (as well as all options for adequate deep underground disposal)

4. Other methods for drilling cutting disposal

It is important to understand the value of an efficient solid control system, because a properly designed and configured one will minimize the overall volume

of drill cutting needing disposal. Formation geology, downhole temperature and pressure, and drilling mud are a few of the inputs to be considered prior to pairing shale shakers, degassers, desanders, and desilters to a solids control system.

The total volume of the cuttings as well as their associated disposal costs can be minimized by tailoring the solids control systems to the well prior to drilling. The most effective way to dispose of cuttings begins with having the least amount of cuttings that require disposal. Therefore, minimization as a waste management method must be a priority to other methods.

Here are the most popular disposal techniques used other than cutting re-injection:

a) **Landfarming:** The process involves spreading drill cuttings on land, and reincorporating into the soil of a licensed property. Landfarming and land treatment permits require the waste to be mixed into the receiving soil via tiling, disking, or plowing, in order to ensure appropriate incorporation of the waste into the soil and prevent the waste migration from the approved disposal site. A disposal site should be chosen where tiling, disking, or plowing of the waste into the receiving soil can be done; otherwise, the site is considered to be unsuitable and an alternative one should be proposed. The disposal process utilizes the physical chemical and biological capabilities of the soil-plant system to control waste migration and to provide a safe means of disposal without impairing the potential of the land for future use. This disposal option is popular and economical.
b) **Biodegradation:** In this technique, cuttings and mud are biologically degraded into simpler components using microorganisms. The process utilizes a nitrogen source for bacterial growth, continual dilution and an odor suppressant. The mixture of cuttings/mud and bacteria should be frequently turned to introduce oxygen to the process. It has been concluded that microbial degradation can be considered as a key component in the cleanup strategy for petroleum hydrocarbon remediation. Currently, biodegradation is considered relatively slow and cannot process large volumes of cuttings.
c) **Solidification:** In this process, disposed cuttings and mud are mixed with a solidification agent such as clay, cement, fly ash and/or lime, to form a concrete-like solid, mechanically binding the cuttings. Solidification of drill cuttings at the wellsite reduces cuttings moisture

content, improving handling and reduces transportation costs. The solid product can be disposed at an authorized disposal site or repurposed for uses such as road aggregate, engineered fill and construction material. This disposal method's usage varies regionally.

d) **Incineration:** This cuttings disposal method is far less frequently used in comparison to other options. In this process, thermal systems are used to burn drill cuttings, typically offshore. It is not a widely used disposal method due to the resulting air emissions, safety concerns of the heat source, and high efficiency required.[12]

Given below is a table (table 2) comparing different drilling waste management techniques. As it is shown, environmental impacts and safety risks of the CRI process, which are the most important factors among others, have low level degree, therefore, its vulnerability as the best option increases to be adopted as the environmentally friendly drilling waste disposal process. Other advantages of the CRI, other than zero discharge, include: having small surface footprint, reduction of the need for waste transportation (via pipelines, marine vessels or tankers onshore), elimination of the risks associated with the surface accumulation of generated waste and is not limited by locations, no future cleanup responsibilities by the operator, full control over the waste management process, worldwide applicability, and being economic. It is simply the lowest cost, easiest course of action for most drilling operations.[1][8]

Comparison Factor	Fixation	Thermal Treatment	CRI	Bioremediation/Composting
Environmental Impact	Low	High	Low	Medium
Cost	\$57-63 per m^3	\$90 per metric ton	\$31 per m^3	\$500 per m^3
Cost factor	May require transport and liner and requires monitoring	Requires transport, air emission control	More expensive if dedicated well(s) are required	May require transport and required monitoring
Safety Risks	High	High	Low	Medium
Technical feasibility	Low	Medium	High	Medium
Liability	Liability may be long-term if there	Little liability	Little liability if	Short term liability while material is treated during

	are subsequent problems with liner, etc.	apart from substances, like heavy metals remaining in the cleaned material	performed correctly	biotreatment, or possible long-term liability if there is subsequent degradation of stabilized material (spreading)

Table 2: Qualitative and quantitative comparison in disposal approaches

Some examples had been given to demonstrate that the cuttings re-injection process is still the most economic method for the disposal of waste generated through exploration and production activities in comparison with other available waste disposal methods. The first example is taken from Port Fourchon Louisiana, where in the period of two years, more than 160 000 m^3 of waste produced by drilling and reduction activities containing naturally occurring radioactive materials, has been injected into a single well with an average cost of $119.5 per cubic meter of waste material, which is far less in comparison with the offsite waste disposal, with an estimated cost of $629 per cubic meter of the same waste material. Similar to the previous example, Marathon Oil Company implemented in the period between 1995 to 2004 a waste slurry injection program and achieved an 89% disposal cost reduction during operations in Alaska (from $337.3 to $36.8 per cubic meter of waste material).[8]

III. ROCK FORMATION AND FRACTURE PROPAGATION STUDY

The starting point for planning an operation or designing any mechanical part that resides in the Cuttings Re-Injection is the study on the site dedicated to this operation. It is necessary to know the type of rock that is found in the subsoil, the existing efforts in the site on which it operates, the possible seismic movements or the presence of any aquifer or reservoir in the surrounding area, the geology of the area, the reservoir characteristics of a target geological rock unit, for example: porosity, permeability, reservoir thickness, reservoir depth, …

- Permeability: The capacity to flow fluids will affect both the fluid leak-off rate from the injected slurry (it will depend on horizontal permeability). The average lower and upper values are: 0.604 and 1.272 μm^2.
- Porosity: The storativity of any geological material depends upon the porosity. High porosity is important to accommodate the liquid phase of the injected waste slurry. The average lower and upper values are 23.8% and 24.7%.
- Thickness and Areal Extent (thickness>20 m): A large thickness and a large areal extent of reservoir rock are necessary to keep induced fractures contained within the target zone, and to help provide sufficient volume of storage for the expelled fluids.
- Reservoir Depth: The injection depth must be sufficient to eliminate all reasonable risk of potable water contamination, yet not so deep as to require massive pumping capability to sustain fracture injection.
- Alternating Sequence of Sandstone and Shale: A shale layer acts as a flow and a stress barrier, whereas a sandstone layer acts as a rapid fluid leak-off zone. An alternating sequence of sandstone and shale will limit upward fracture growth.
- Geographical Distance: The geographical distance between a waste disposal and a waste collection site should be short; which will make the injection operation economical and more environmentally secured (reduced transportation risk)

- Cap Rock and its Thickness: A thick layer of cap rock (low permeability strata) will act as a confining unit above the reservoir rock. It represents a flow and stress barrier.
- Reservoir Strength: An ideal reservoir rock should be weak in tension (low cohesion or intensely fractured); it will then offer less resistance against breaking at low values of effective stress.
- Reservoir Compressibility: A highly compressible rock will more easily produce thick (wide aperture) fractures during injection; therefore, it will more easily accommodate large volumes of solid waste.
- Structural/Tectonic History: A structurally and tectonically passive disposal site will more securely contain injected waste in the target stratum by eliminating the chances of upward fluid migration paths through pre-existing fractures and faults

Cuttings disposed by CRI technique should be placed into a target formation which is composed of poorly consolidated sands. This formation should have all the properties mentioned above. Poorly consolidated sand is chosen as a target formation because it is characterized by a high porosity which provides more pore space volume into which solids can be placed than formations with low porosity. In addition, poorly consolidated formations have high compressibility, which means it can be displayed easily during hydraulic fracturing to create more volume for waste placement. Above the target formation should be a confining zone which is composed of shales. The shales should be relatively impermeable and at least of 20 to 50 m in thickness; this zone should also be extensive in area (>25 km^2) and relatively uniform in properties throughout this area. As for the sands, it should have a sufficient permeability to absorb any upward fluid motion. Shales tend to limit fracture growth since they have higher horizontal stresses than sands and have higher stiffness. Thin sands would limit fracture growth since fracture fluid drains rapidly into them instead of remaining in the fracture. Mechanical slippage at the sand-shale interface may also halt the upward growth of a fracture tip.

1. Rock mechanics: Stresses and deformations of the rock

Rock mechanics involves the investigation of the deformation of in-situ rock material resulting from natural and external loading processes. Thus, load and deformation form the basis of rock mechanics. The most useful principles of rock mechanics are based on data obtained from laboratory testing and in situ measurements used in conjunction with the basic concepts of solid mechanics to quantify the behavior of rock to various disturbances.

a) Stresses

When considering the force acting on any portion D of a continuum body C, we have to distinguish between two types of forces:

1-Those forces acting on D from the exterior of C, called body forces, such as mass forces, represented by a vector field b

2-Those forces interior to C and acting on the boundary ∂D of the portion D, called contact forces.

Contact forces are associated with the specific surface we choose at a given point. We consider a body subjected to external forces P1, P2, P3 as sketched in fig.3. If the body is divided into two parts by an arbitrary plane π through the point P and one of these parts is removed, the equilibrium of forces will no longer be satisfied, unless the system of internal forces is specified. This system represents the contact forces exerted by one part onto the other. It is assumed that the actions on the small element of surface dA, oriented by the unit outward normal vector n, can be reduced to the vector df, applied at the point P, and postulated that the limit:

$$\lim_{dA \to 0} \frac{df}{dA} = \sigma \quad \textit{(eq.1)}$$

exists and is finite. The vector σ is called stress vector. This vector depends in general on the surface on which the point P lies, so that if we consider a different surface at the same point, the stress vector will in general be different.

To give a complete description of the stress state at a point P within a sample, it is necessary to identify the stresses related to surfaces oriented in three orthogonal directions. The stresses related to a surface normal to the x-axis may be denoted σ_x, τ_{xy} and τ_{xz}, representing the normal stress, the shear stress related to a force in y-direction, and the shear related to a force in the z-direction, respectively.

Similarly, the stresses related to a surface normal to the *y*-axis are denoted σy ,τyx and τyz, while the stresses related to a surface normal to the *z*-axis are denoted σz, τzx and τzy .Thus, there are all together nine stress components related to the point P:

$$\begin{pmatrix} \sigma x & \tau xy & \tau xz \\ \tau yx & \sigma y & \tau yz \\ \tau zx & \tau zy & \sigma z \end{pmatrix}$$

This expression is called the stress tensor. It gives a complete description of the stress state at the point P.

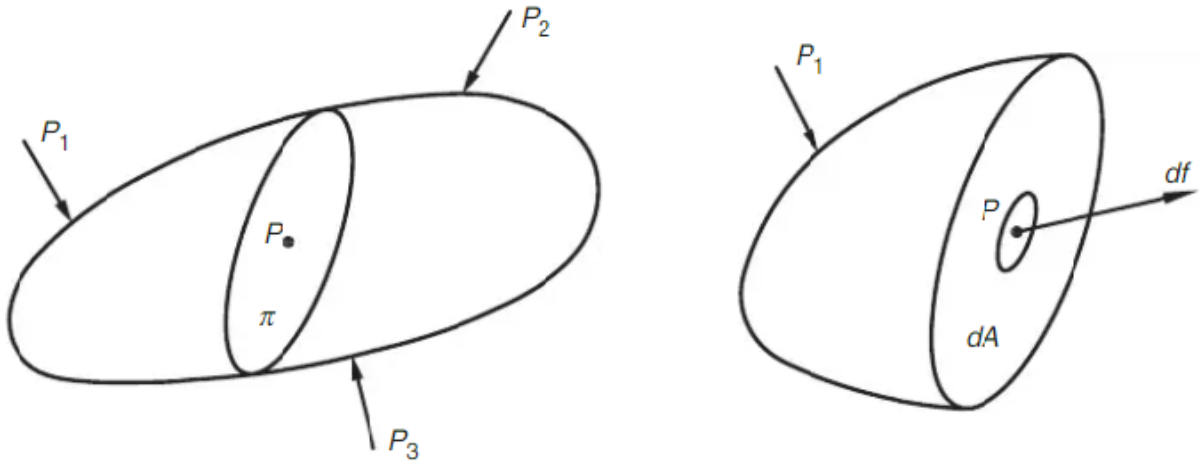

Fig.3: The concept of stress

b) Strain

If we consider a particle within a sample, its position is initially x, y, z. After the application of an external force, the position of this particle will be shifted. The shift in the x-direction is denoted by u, in the y-direction by v, and in the z direction by w. If the displacements u, v and w are constants (that means they are the same for every particle within the sample), then the displacement is a translation of a rigid body. Another simple form of displacements is the rotation of a rigid body.

If the relative position of the particles within the samples are changed, so that the new positions cannot be obtained simply by a rigid translation and/or rotation of the sample, the sample is said to be strained. An example of a strained sample is shown in figure 4. The displacements related to the positions O and P are not equal. The quantity defined as

$$\varepsilon = \frac{L - L'}{L} = -\frac{\Delta L}{L} \ (eq.2)$$

is called the elongation corresponding to the point O and the direction OP.

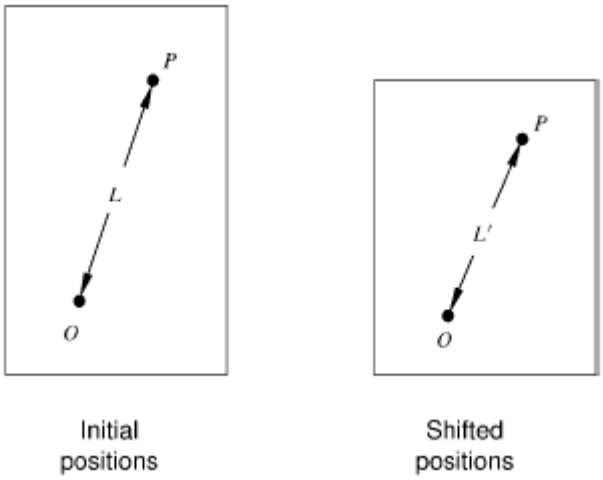

Fig.4: Deformation

The elongation is a specific type of quantities known as strains. The other type of strain that may occur can be expressed by the change Ψ of the angle between two initially orthogonal directions (Fig.5).

$$\tau = \frac{1}{2} \ tan \ \Psi \ (eq.3)$$

This quantity is called shear strain corresponding to the point O and the direction OP.

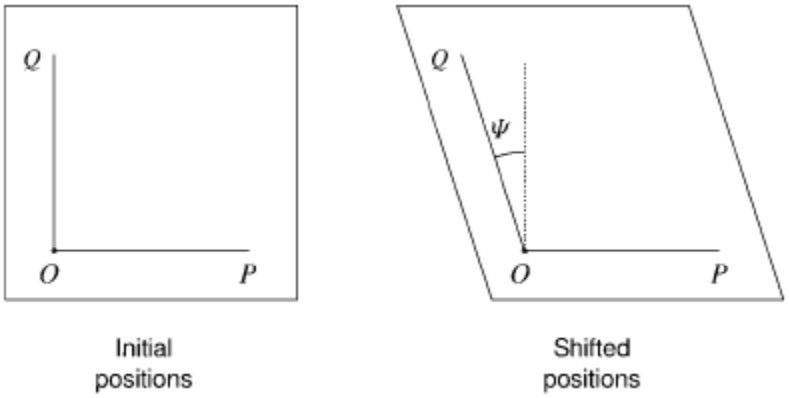

Fig.5: Shear deformation

To give a full description of the strain state at a point within a three-dimensional body, the elongations and shear strains corresponding to all three axes must be specified.

Similar to stresses, strains can be organized in a strain tensor:

$$\varepsilon=\begin{pmatrix} \varepsilon x & \tau xy & \tau xz \\ \tau xy & \varepsilon y & \tau yz \\ \tau xz & \tau yz & \varepsilon z \end{pmatrix}$$

we can pose the problem of finding a local reference system in which the shear stresses vanish. In this case the coordinate axes are called principal axes and the coordinate planes are called principal planes. The stress vector acting on a principal plane is characterized by only the normal component. The principal stresses are given by: σ_1, σ_2, σ_3. The components of the stress tensor at a point will change in different coordinate systems, but the three principal stresses are invariant under coordinate transformation. Furthermore, if we choose a coordinate system such that the coordinate directions are parallel to the principal directions, in that system the stress tensor representation takes the form [43]:

$$[\sigma_{ij}] = \begin{bmatrix} \sigma 1 & 0 & 0 \\ 0 & \sigma 2 & 0 \\ 0 & 0 & \sigma 3 \end{bmatrix}$$

c) In situ stresses

In situ stresses are considered as important parameters, especially in the oil and gas industry. Generally, in situ stresses include three mutually orthogonal principal stresses in the subsurface, which are known as the vertical (overburden) stress and the maximum and minimum horizontal stresses. Three in situ stresses correspond to three principal stresses: the greatest stress σ_1, the intermediate stress σ_2, and the smallest stress σ_3. Three in situ stress regimes can be used to describe the in-situ stress field according to the relationship of the three principal stresses. When an opening is excavated in the rock, the stress field is locally disrupted and a new set of stresses are induced in the rock surrounding the opening. The determination of the in-situ stresses is shown below.[20]

A rock at depth is subjected to stresses resulting from the weight of the overlying strata and from locked in stresses of tectonic origin.

If we consider an element of rock at a depth of 1000 m below the surface, the weight of the vertical column of rock resting on this element is the product of the depth and the unit weight of the overlying rock mass. Hence, the vertical stress on this element is given by the simple relation:

$$\sigma_v = \gamma.z \quad (eq.4)$$

where γ is the unit weight of the overlying rock expressed in MN/m^3 and z is the depth below the surface expressed in meters.

The horizontal stresses acting on an element of rock at a depth z below the surface are much more difficult to estimate than the vertical stresses [10]. Normally, the ratio of the average horizontal stress to the vertical stress is denoted be the letter *k* such that:

$$\sigma_h = k.\ \sigma_v = k.\gamma.z \quad (eq.5)$$

where *k* is the coefficient of earth pressure at rest in terms of effective stresses. This coefficient contains the words 'at rest' since the soil was deposited under conditions of zero horizontal strains. In other words, because of the large lateral extent of the soil deposit, the vertical planes on any soil element A do not experience any lateral movement as the stresses increase as a consequence of the accretion of material on the ground surface.

The value of *k* can be determined if the soil is assumed to behave as an elastic solid, as follows:

$$\varepsilon_H = \frac{1}{E}(\sigma_H - \nu\ \sigma_v - \nu\ \sigma_H) = 0 \quad (eq.6)$$

where ε_H = horizontal strain

E, ν = elastic parameters for soil

From the equation above, *k* will be equal to $\frac{\nu}{1-\nu}$, which indicates that *k* varies from 0 to 1 as the Poisson's ratio varies from 0 to 0.5.

The assumption of elastic behavior for many soils may be an unrealistic idealization so the value of *k* should be determined experimentally. In the laboratory, *k* can be determined by applying a vertical stress σ_v to a soil sample while preventing all horizontal movement. The value of the horizontal stress (σ_H) required to prevent this movement is measured. The value of *k* is then calculated from the measured value of σ_H and the applied value of σ_v. [11]

The equation of k was widely used in the early days of rock mechanics. It was proven to be inaccurate and is seldom used today. Measurements of horizontal stresses around the world show that the ratio k tend to be high at shallow depth and decrease at increasing depth. A model was given by Sheorey (1994), in which he developed an elasto-static thermal stress model of the earth. The model considers curvature of the crust and variation of elastic constants, density and thermal expansion coefficients through the crust and mantle. It provides a simplified equation that can be used for the estimation of the horizontal to vertical stress ratio k. This equation is given by:

$$K = 0.25 + 7E_h(0.001 + \frac{1}{z}) \quad (eq.7)$$

Where z is the depth below surface expressed in meters, and E_h is the average deformation modulus of the upper part of the earth's crust measured in a horizontal direction and expressed in GPa. In layered sedimentary rock in particular, this direction of deformation is considered is considered important, in which the deformation modulus may be significantly different in different directions [21].

d) Pore pressure and effective stress

Formation pore pressure is the pressure exerted by the formation fluid on the walls of the rock pores. A part of the overburden stress is supported by the pore pressure, while the other part is taken by the rock grains.

Based on the magnitude of the pore pressure gradients, formations can be classified. In general, two types of formation pressure are known:

- Normal formation pore pressure (hydropressure): It is when the formation pore pressure is equal to the hydrostatic pressure of a full column of formation water. Normal pore pressure is usually of the order of 0.465 psi/ft
- Abnormal formation pore pressure (geo-pressure): Abnormal pore pressure exists in regions where there is no fluid that directly flows to the adjacent regions. Having impermeable boundaries, the fluid cannot flow and will be trapped to take large proportion of the overburden stress. Abnormal formation pore pressure is usually ranged between 0.8 and 1 psi/ft.

The pore pressure should be calculated for the study of fracturing. This could be done by using a simple method, which is the Eaton's equation:

$$G_p = G_{sed} - (G_{sed} - 1.03)\left(\frac{\Delta T_{NCT}}{\Delta T_{calc}}\right)^n \quad (eq.8)$$

This equation is based on the ratio between the normal ΔT, ΔT_{NCT} that is read on the normal compaction trend line, and the computed value, ΔT_{calc}.
n depends on the method used to define the normal compaction trend line and can be usually taken equal to 3 if the sonic log has been evaluated (or seismic data); or equal to 1.5 if a resistivity log has been considered.
G_p and G_{sed} are respectively the pore and overburden gradients
The effective stress at any point on or near the borehole is generally described in terms of three principal components. It is a radial stress component that acts along the radius of the wellbore, a hoop stress acting around the circumference of the wellbore (tangential), and an axial stress acting parallel to the well orientation, and an additional shear component.

A rock is a porous material that consists of a fluid and a rock matrix. The overburden stress is supported by the pore pressure and partly by the rock matrix. Therefore, the total stress is equal to the pore pressure plus the effective as stated in the following equation:

$$\sigma = \sigma' + P_0 \quad (eq.9)$$

The rock failure analysis is governed by the following stress known as effective stress:

$$\sigma' = \sigma - P_0 \quad (eq.10)$$

A fluid at rest cannot transmit shear stresses, so the effective stress is valid for normal stresses, and therefore, shear stress remains unchanged (Terzaghi, 1943)

A more general representation of the effective stress includes a scaling factor with respect to the pore pressure, which is known as the Biot's constant.

This is expressed by:

$$\sigma' = \sigma - \beta P_0 \quad (eq.11)$$

where:

$$\beta = 1 - \frac{E}{Ei}\frac{1-2\nu i}{1-2\nu} = 1 - \frac{Porous\ Matter}{Interpore\ Material} \quad (eq.12)$$

where E is the modulus of elasticity, n is the Poisson's ratio, and index I refers to the interpore material, and the remaining terms to the bulk material. For real rocks, the Biot's constant may range between 0.8 and 1.

The properties of the formation in which the CRI operation will take place, such as the Poisson ratio, the Young modulus, the state of stress, the pressure, … are already known based on past work in the formation. In case some parameters should be checked, samples could be taken and examined in the laboratory, or another method is the use of sonic logs, resistivity logs, density logs, MDT and DST tools, …

2. Failure mechanics

By rock failure, we mean the formation of faults and fracture planes, crushing, and relative motion of individual mineral grains and cements. When a piece of rock is subjected to sufficiently large stresses, a failure of some kind will occur. Fracturing caused by the CRI operation is considered to be a tensile failure. In the next parts, we will describe all the three types of failures: Tensile Failure, Shear Failure, and Compaction Failure.

a) Tensile Failure

Tensile failure occurs when the effective tensile stress across some plane in the rock exceeds a critical limit. This limit is called the tensile strength, given the symbol T_0, and has the same unit a stress. The tensile strength is a characteristic property of the rock. Most sedimentary rock has low tensile strength, typically only a few MPa or less. For several applications, the tensile strength is assumed to be equal to zero.

A rock that suffers from tensile failure splits along one or very few fracture planes, as shown I figure 6. Thus, tensile failure is a highly localized and inhomogeneous process. The fracture planes often originate from preexisting cracks, oriented more or less normal to the direction of the tensile stress. The largest crack(s) will grow increasingly faster than the other, and rapidly split the rock.

The failure criterion, which specifies the stress condition for which tensile failure will occur, and identifies the location of the failure surface in principal stress space, is given as:

$$\sigma' = -T_0 \quad (eq.13)$$

For isotropic rocks, the conditions for tensile failure will always be fulfilled first for the lowest principal stress, so that the tensile failure criterion becomes:

$$\sigma'_3 = -T_0 \quad (eq.14)$$

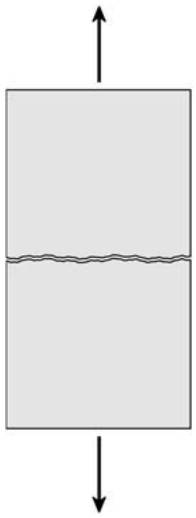

Fig. 6: Tensile failure

b) Shear failure

Shear failure occurs when the shear stress along some plane in the sample is sufficiently high. Eventually a fault zone will develop along the failure plane, and the two sides of the plane will move relative to each other in a frictional process, as shown in figure 7.

The frictional force that acts against the relative movement of two bodies in contact depends on the force that presses the bodies together. So, it is reasonable to assume that the critical shear stress (τ_{max}) for which shear failure occurs, depends on the normal stress (σ') acting over the failure plane. That is:

$$|\tau max| = f(\sigma') \qquad (eq.15)$$

This assumption is called Mohr's hypothesis.

In the τ- σ' plane, this equation describes a line that separates a 'safe region' from a 'failure region'. This line is sometimes referred to as the failure line or the failure envelope. An example is shown in figure 8, where the three principal stresses and the Mohr's circle connecting them are shown. For a given set of principal stresses, all possible combinations of τ and σ' lie within the area in between the three circles (the shaded are of figure 8).

The stress state in figure 8 represents a safe situation, as no plane within the rock has a combination of τ and σ' that lies above the failure line. If the σ_1' increases, the circle connecting σ_1' and σ_3' will expand, and eventually touch the failure line. The failure criterion is then fulfilled for some plane(s) in the sample, and the sample fails. We note that the value of the intermediate principal stress (σ_2') has no influence on this situation. Since σ_2' by definition lies within the range (σ_3', σ_1'), it does not affect the outermost of Mohr's circles, and hence it does not affect the failure. Thus, pure shear failure, as defined by Mohr's hypothesis, depends only on the minimum and maximum principal stresses and not on the intermediate one.

By choosing specific forms of the function $f(\sigma')$, various criteria for shear failure are obtained. The simplest possible choice is a constant. The resulting criterion is called the Tresca criterion, it states that the material will yield when a critical level of shear stress is reached:

$$\tau_{max} = \frac{1}{2}(\sigma_1' - \sigma_3') = S_0 \quad \textit{(eq.16)}$$

S_0 is the 'inherent shear strength' (also called 'cohesion') of the material. In a Mohr τ – σ' plot, the Tresca criterion appears simply as a straight horizontal line.

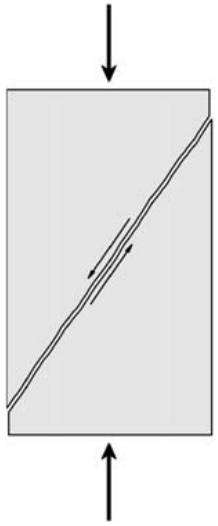

Fig. 7: Shear failure

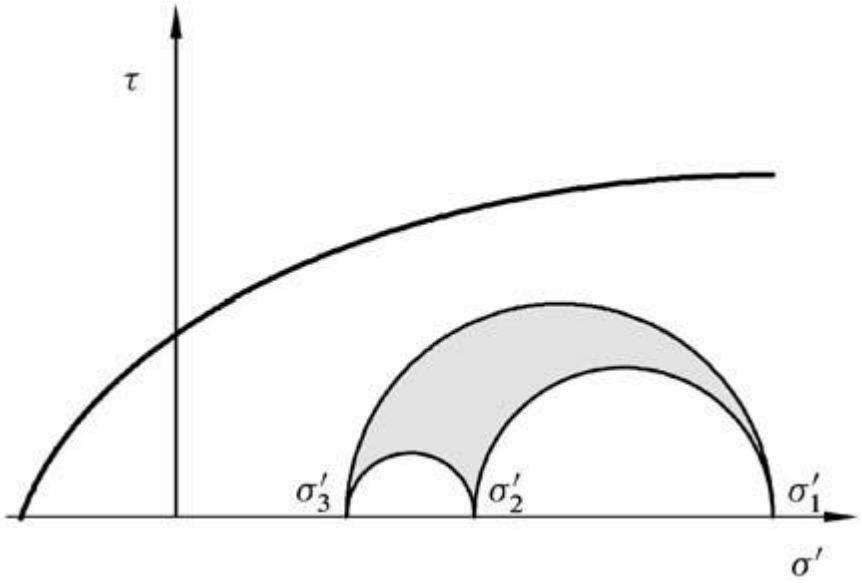

Fig.8: Failure line as, in the shear stress-normal stress diagram. Also shown are the Mohr circles connecting the principal stresses σ_1', σ_2', σ_3'.

The two other criterion of shear failure are: - The Mohr-Coulomb criterion

- The Griffith criterion

The Mohr-Coulomb criterion is more general and frequently used. It is based on the assumption that $f(\sigma')$ is a linear function of σ':

$$|\tau| = S_0 + \mu\, \sigma' \quad \textit{(eq.17)}$$

Where μ is the coefficient of internal friction.

A failure criterion was developed by Griffith based on a study of elliptical microcracks in a two-dimensional model. When the tensile stress at the tip of the crack exceeds a certain characteristic value of the material, the crack will grow and the failure process will be initiated. The theory is scaled in terms of the uniaxial tensile strength T_0, and the resulting failure criterion will be written as:

$$(\sigma_1' - \sigma_3')^2 = 8T_0((\sigma_1' + \sigma_3') \qquad \text{if } \sigma_1' + 3\,\sigma_3' > 0 \quad \textit{(eq.18)}$$

$$\sigma_3' = -T_0 \qquad \text{if } \sigma_1' + 3\,\sigma_3' < 0 \quad \textit{(eq.19)}$$

the criterion is represented by a parabola ending in a straight line in a principal stress plot.

The uniaxial compressive strength C_0 is given by: $C_0 = 8T_0$.

c) Compaction failure

In high porosity materials, it is normally observed that the pore collapse is the type of failure mode, where the grain skeleton forms a relatively open structure. In a material under compression, the grains may loosen or break and then be pushed or twisted into the open pore space, which results in a closer packing of the material. This deformation mode is called compaction and is illustrated in figure 9.

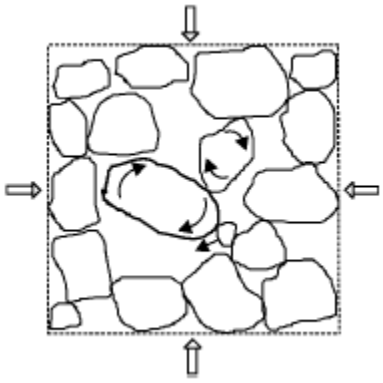

Fig.9: Grain reorientation resulting in a closer packing

Pore collapse may occur under pure hydrostatic loading. Microscopically, the local excessive shear forces acting through grains and grain contacts will cause the

failure. From this perspective, pore collapse may be regarded as distributed shear failure within the material.

Also grain failure is another failure mechanism that could occur under hydrostatic loading. Under sufficiently high stresses, at the grain contact, the grains may be partly crushed, and they endure splitting. These local failure mechanisms represent permanent damage of the rock framework and causes yielding, with reduction in rock stiffness. This type of failure may also occur under non-hydrostatic stress conditions, like in triaxial tests at high confining pressure. In this case, the process will be referred to as shear-enhanced compaction.

3. Elasticity

Most materials have an ability to resist and recover from deformations produced by forces. This ability is called elasticity. It is the foundation for all aspects of rock mechanics. The simplest type of response is one where there is a linear relation between the external forces and the corresponding deformations. When changes in the forces are sufficiently small, the response is (nearly) always linear. Thus, the theory of linear elasticity is fundamental for all discussions on elasticity.
The theory of elasticity rests on the two concepts stress and strain.
The region of validity for linear elasticity is often exceeded in practical situations. In petroleum related rock mechanics, much of the interest is furthermore focused on rocks with a significant porosity as well as permeability. The elastic theory for solid materials is not able to fully describe the behavior of such materials, and the concept of poroelasticity has therefore to be taken into account. The elastic response of a rock material may also be time dependent, so that the deformation of the material changes with time, even when the external conditions are constant.
In this work, the deformation of the rock is considered to be elastic.

4. Poroelasticity

Rocks are generally composite materials, hence inhomogeneous on a microscopic scale. The way rocks behave, their elastic response, their failure stresses, … depend, to a large extent on the non-solid part of the material. The non-solid part is represented by the pore space in the rock which is not only essential

for oil to be produced from a reservoir, bur also plays an important role in a rock mechanical behavior. Poroelasticity is the term used to describe the interaction between fluid flow and solids deformation within a porous medium. When an external load is applied to a porous medium, the volume fraction of the pores is affected. The fluid-filled pores experience a change in pressure under this mechanical stress, which leads to fluid motion. As a reaction to this change in pore volume, the solid material shifts and deforms elastically [15]. The theory of poroelasticity was introduced by the pioneering work of Biot (1941). The theory was originally developed for soil mechanics, especially for consolidation problems. For the definition of poroelastic system, five material constants are required: the shear modulus G, the drained Poisson ratio n, the undrained Poisson ratio V_u, the Skempton pore pressure coefficient B, and the intrinsic permeability K. These constants have been successfully linked to micromechanical parameters that can be easily obtained for any soil or rock type material. These micromechanical parameters are given by the porosity n, the fluid bulk modulus K_f, the solid grain bulk modulus K_s, the porous bulk modulus for the solid skeleton K, the Poisson ratio n, and the permeability k.

The total stresses σ_{ij} are related to the effective stresses σ'_{ij} through:

$$\sigma_{ij} = \sigma'_{ij} - \alpha p \quad \textit{(eq.20)}$$

the effective stresses govern the deformation and failure of the rock. The poroelastic constant α is independent of the fluid properties, and is defined as:

$$\alpha = \frac{3(\upsilon\upsilon - \upsilon)}{B(1-2\upsilon)(1+\upsilon\upsilon)} = 1 - \frac{K}{Ks} \quad \textit{(eq.21)}$$

It is important to consider the compressibility of the constitutive materials when applying this formulation to the rock. For soils, B and αare equal to unity, but in rocks, they are significantly less than one.

The theory of poroelasticity can be approximated numerically using the finite element method and a standard Galerkin formulation as described in Zienkiewicz and Taylor (1991) and Lewis and Schrefler (2000).[16]

5. Mechanics of fracture initiation and propagation

Hydraulic fracturing in rocks takes place when the fluid pressure within the rock exceeds the smallest principal stress plus the tensile strength of the rock. This results in tensile failure or splitting of the rock. Artificial or man-made fractures are initiated by increasing the fluid pressure in the borehole to the point where the smallest principal stress at the borehole becomes tensile. Elevated pressures due to continuous pumping will cause the formation to split and the fracture to grow in the least resistance direction. At distances far from the borehole, the fracture will propagate in the direction normal to the smallest principal stress in the specific formation. As the least principal stress is often in a horizontal direction, the resulting fractures will be vertical, as illustrated in figure 10 in case of a vertical open hole, where two symmetric fracture wings develop perpendicularly to the least principal stress.

Except for short term single-event injection episodes, long term CRI does not result in the propagation of classical single-planar fractures. So, the evolution from single-planar fracture is obtained by repeated injection episodes, and the relatively high injected volumes.

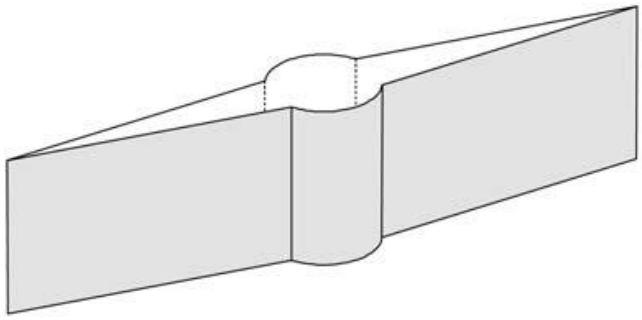

Fig.10: Vertical fracture around a vertical well

Deviating from a single-planar fracture is caused by the clogging of the tip of the fracture with injected solids to the point where it becomes easier for the fracture to continue as a branch off of the main fracture. Initially, the branched fractures will tend to re-align themselves parallel to the main fracture as shown in figure 10. However, as repeated injection episodes are made, the stress field within

the disposal domain alters to the point at which the direction of the least principal stress re-equilibrates. In the case of a vertical fracture, the azimuth of the newly propagating fractures will change. With continued injection, it is possible that the least principal stress field becomes vertical, which could cause fractures to propagate horizontally. This could represent an advantage by eliminating the vertical containment concerns.

Much of the subsequent treatment of fracture will be based on the elastic solutions of the stresses near the tip of the crack. The coordinate axes in figure 11 are located at the tip of the crack, which extends through the thickness of the plate. The crack lies along the negative x-axis, the y-axis is normal the plane of the crack, and the z-axis coincides with the leading edge of the crack. Three crack displacement modes can be distinguished: *Mode I* or direct opening (or tensile) loading shown in figure 11, where the fracture surfaces separate symmetrically with respect to the crack plane; this mode could be applied to the majority of fracture problems (it is the most commonly encountered), and the stresses near the crack tip will be defined for this case; also, the fracture toughness and fracture energy for this mode are cited for most situations. *Mode II* is a sliding (or in-plane shearing) mode, where the fracture surfaces slide symmetrically with respect to normal, but asymmetrically with respect to the crack plane; it occurs less frequently. *Mode III* is a tearing mode, described as antiplane strain or sideways shear, where the fracture surfaces slide asymmetrically with respect to both the crack plane and its normal; it is the easiest of the modes to analyze, especially if plastic as well as elastic deformation is involved. The fracture of a material may involve either one or a combination of the three crack displacement modes; combinations of Mode I and Mode II arise when the loading axis is inclined to the plane of the crack.

In the case of fractures induced by cuttings re-injection operation, the fracture will follow *Mode I.* [18][19]

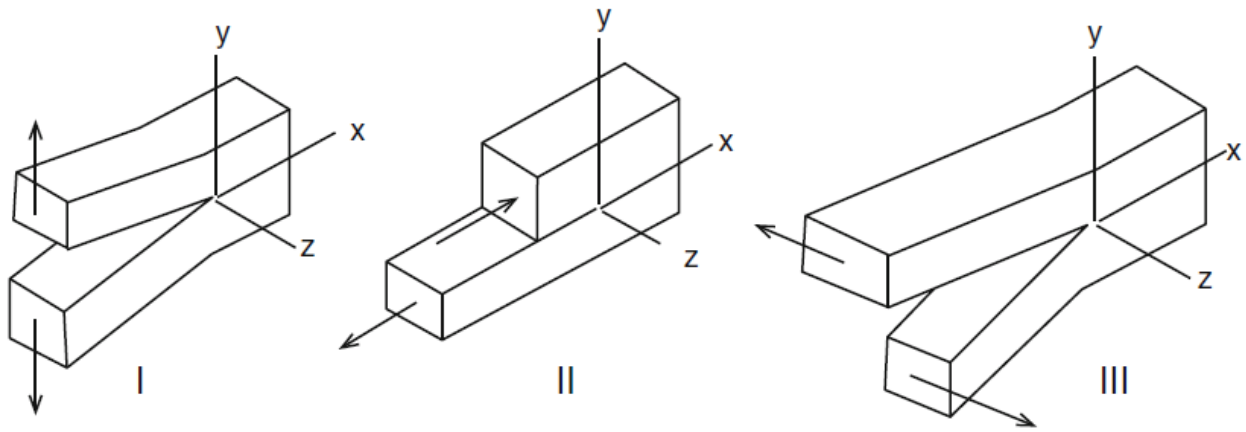

Fig. 11: The basic modes of crack surface displacement

i. Introduction

The design of a CRI operation to create fractures depends on the presence or absence of natural fractures in the reservoir. Fracturing the formation without the presence of natural fractures is based on the assumptions that the rock is homogenous, isotropic and often elastic, and that the fractures propagate symmetrically in a plane perpendicular to the minimum principal stress. As mentioned above, fractures initiate on the wellbore wall when the principal tensile stress within the rock (due to the fluid pressure within the rock) exceeds the minimum principal stress plus the tensile strength of the rock (according to the tensile strength criterion).

If the target rock contains geologic discontinuities, this may alter the initiation, propagation and geometry of hydraulic fractures in a way that is possible in homogenous and isotropic media. Some experimental investigations have demonstrated that the advancing induced fractures during the slurry injection could cross the natural fracture without any significant change in its direction, turn into the natural fracture and dilate it, or, in some cases turns into the natural fracture and beside the dilation of natural fracture, it breaks out again by a fracture or flaw along the natural fracture. Originally, it depends on the orientation of the natural fracture relative to stress field (Blanton 1982; Daneshy 1974; Lamont & Jessen 1963). Considering the experimental results in a multifractured medium, it was observed that the fracture geometry is a function of horizontal differential stress, stress regime, flow rate and discontinuity pattern. Also, it has been concluded that the distribution of crustal stress, the stress state around the wellbore and the types of the targeted formation are the important factors that influence fracture initiation.

Furthermore, many field experiments have been conducted to examine the influence of natural fractures on the propagation of the induced fracture. These studies have demonstrated that the encounter between the propagating fracture and the pre-existing natural one may lead to arrest of the fracture propagation, fluid flow into discontinuities and enhanced fluid leak-off, creation of multiple fractures and fracture offsets which result in a reduced fracture length and fracture width locally at least. Local fracture width reduction may cause cuttings bridging and pre-mature screen-out.

Since the fracture growth from the wellbore during fracturing is considered to be a crack growth problem, it is necessary to use the fracture mechanics framework to investigate the crack growth behavior of the fractures. From the fracture mechanics principles, very high intensity of stresses at crack tip, which can govern initiation then propagation of the fracture, is characterized mainly by the stress intensity factors K_I, K_{II}, and K_{III}. Surely, the onset of fracture initiation and the trajectory of growing fracture can be predicted by the fracture parameters of the initial crack; that means at the onset of wellbore fracturing the crack tip stress intensity factors reach their critical values which result in growth of a fracture through the rock formation. In some researches, it was revealed that the onset of fracture initiation and the trajectory of the fracture can be estimated by determining the crack tip parameters of the perforated wellbore using:

i. The numerical simulations of wellbore using finite element models,
ii. Determining the fracture toughness of the rock (by coring from the site location then testing them using available fracture toughness testing methods),
iii. Employing theoretical fracture criteria for predicting the behavior and path of growing crack.

ii. Fracture initiation

A fracture created by the slurry injection will first occur at a point on the boundary of the wellbore where the effective stress equals or exceeds the tensile strength σ_t of the rock. When the vertical fracture is initiated, it will propagate in the perpendicular to the least effective principal stress, as long as enough fluid is

pumped into it. The vertical fracture will initiate and propagate in both directions symmetrically. That means by increasing the fluid pressure in the wellbore to the point where the minimum principal stress at the borehole becomes tensile, the fracture will be initiated. Continued pumping of the slurry at an elevated pressure will cause the rock to split and the fracture to propagate in the direction of the least resistance.

The initiation of the fractures at the wellbore wall is affected by the stress concentration around the well, and the orientation of the fracture as it propagates is controlled by the manner in which the minimum principal stress is oriented away from the well.

i. Borehole pressure

Assuming a homogenous, linearly elastic, isotropic rock mass, the stresses around the wellbore could be expressed as:

$$\sigma_r = P_p \quad \textit{(eq.22)}$$

$$\sigma_{\Theta\Theta} = \sigma_x + \sigma_y - 2(\sigma_x - \sigma_y)\cos 2\Theta - P_w - 4\tau_{xy}\sin 2\Theta \quad \textit{(eq.23)}$$

$$\sigma_{z\Theta} = \sigma_z - 2\nu(\sigma_x - \sigma_y)\cos 2\Theta - P_w - 4\nu\tau_{xy}\sin 2\Theta \quad \textit{(eq.24)}$$

$$\tau_{r\Theta} = \tau_{rz} = 0 \quad \textit{(eq.25)}$$

$$\tau_{\Theta z} = 2(-\tau_{xz}\sin\Theta + \tau_{yz}\cos\Theta) \quad \textit{(eq.25)}$$

where σ_r is the radial stress, $\sigma_{\Theta\Theta}$ is the tangential stress and $\sigma_{z\Theta}$ is the axial stress at angular position Θ on the wellbore.

The shear stresses τ_{xy}, τ_{yz}, τ_{zx} are acting on the wellbore in a rectangular coordinate system while $\sigma_{r\Theta}$, σ_{rz}, $\sigma_{\Theta z}$ are acting in a cylindrical coordinate system. P_p is the pore pressure and Θ is the angular position. The stresses σ_x, σ_y, σ_z are the normal stresses on the borehole. The single subscript means the direction of the stress. The stresses with two subscripts are interpreted as follows: the first index refers to the location of a stress on the plane which has an outward normal parallel to the axis, and the second one refers for the direction where it acts along. This stress distribution around the wellbore is shown in figure 12. A detailed explanation of the stresses in the rectangular coordinate system can be derived from the in-situ principal stresses (Hossain, et al. 2000).

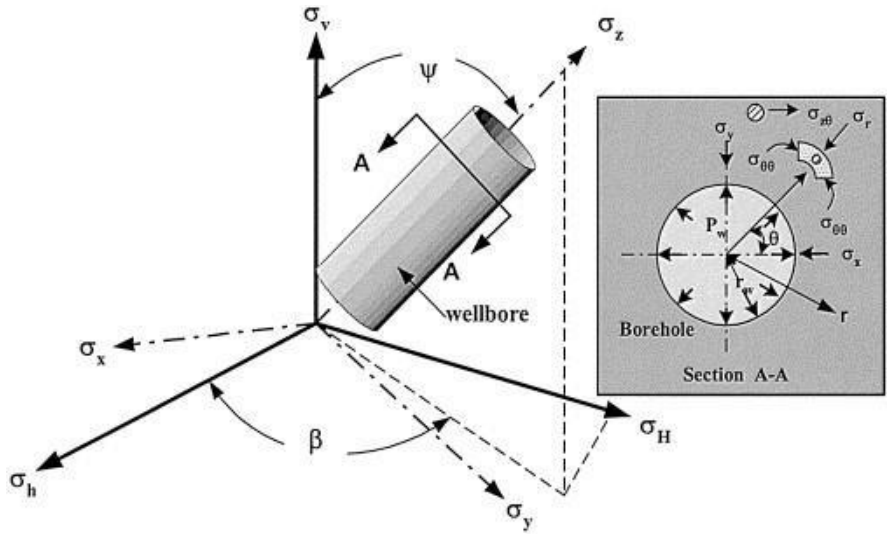

Fig. 12: A random borehole in an in-situ stress regime, stresses around the borehole are displayed.

Figure 13 display the stresses acting around an open vertical borehole in a rock. σ_v which is the vertical stress has the greater value and it remains constant in the rock. The stress σ_r first is equal to the wellbore pressure and then it declines with increasing the distance from the borehole. For $\sigma_{\Theta\Theta}$, it is the opposite; ti increases with higher distance. Both stresses are equal to the minimum horizontal stress in the far field. It is assumed that the pore pressure P_p is unaffected by the borehole pressure P_w.

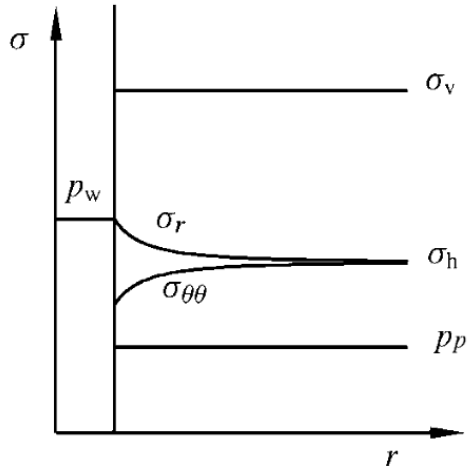

Fig. 13: Stresses distribution around a borehole assuming axisymmetric virgin stress field. The borehole is open, vertical and in an impermeable rock mass (modified from Fjaer et al. 2008)

ii. Fracture initiation

Fracture propagation is governed by the mechanical properties of the injection zone and surrounding formations. During slurry injection, the surface injection pressure must be carefully observed, to avoid undesirable or rapid injection pressure build-up that could jeopardize the operational life of an injection well and limit its waste disposal capacity. Usually, the waste disposal domain in a slurry fracture injection is idealized with a "wagon-wheel" uniform multi-fracture domain (Figure 14a), with multiple fractures of uniform width or uniform strain [56]. But, according to Ji et al. [51] and Shokanov et al. [78], it was found that a "wagon-wheel" multi-fracture disposal domain is not a general case in cuttings injection, and in some cases, it is more likely to reopen the existing fracture and increase it or make a branch from it than to create a new fracture with a different azimuth (Figure 14b,c). Willson et al. in 1999 [25] conducted a comprehensive laboratory research related to the fracture formation in different types of rocks and observed a formation of multiple fractures in the majority of examined rock (formation) samples as a result of an intermittent injection process. The appearance of formation damage during the batch slurry waste injection and consequent change of the formation leak-off properties can directly affect the fracturing process and propagation of the disposal domain. If a new fracture or branch is created with each newly injected batch volume, the leak-off properties and the formation damage will depend on the proportion of the formation damage from previous injections. It was concluded that, in large-scale injection projects, multiple fractures are likely to occur as a result of reduction in the fracture conductivity in combination with a stress increase within the waste pod. Additionally, with every newly injected volume during the intermittent injection process, a new fracture will be created with a variation in azimuth between 30° and 60° compared to the previous one [40]:

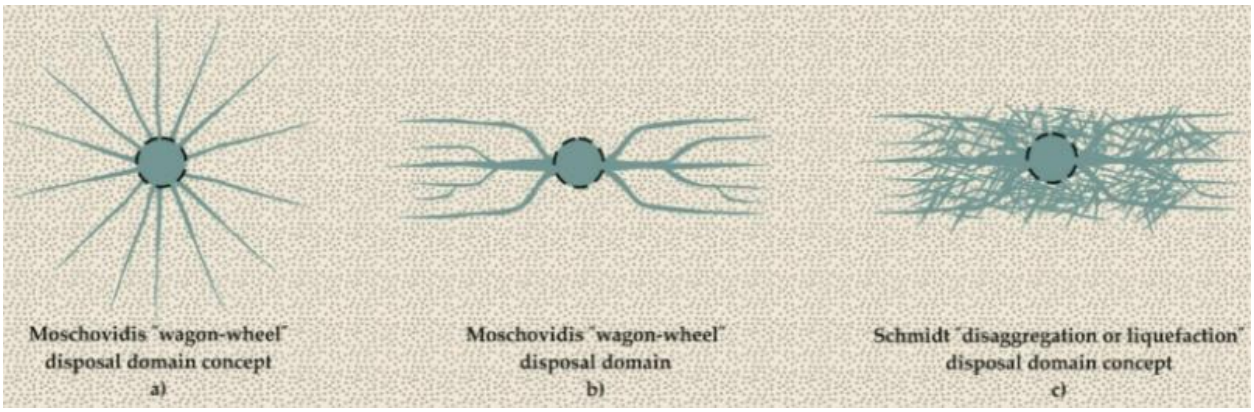

Fig. 14: Different models for characterization of a disposal domain

As the rate of fluid loss at the growing fracture tip is extremely high, it is not possible to initiate a fracture with the slurry containing the drilling cuttings because the high fluid loss would cause the cuttings at the fracture tip to reach the consistency of a dry solid, which causes bridging and screen out conditions. Consequently, water must be pumped before the slurry is pumped to initiate the fracture [23].

For a non-perforated wellbore, a fracture will initiate according to the failure criterion given by Griffith, when a principal tensile stress reaches the tensile strength of the rock. The three principal stresses are calculated as follows:

$$\sigma_1 = \sigma_r \quad \textit{(eq.26)}$$

$$\sigma_2 = \frac{1}{2}\left[(\sigma_{\Theta\Theta} - \sigma_{z\Theta}) + \sqrt{(\sigma_{\Theta\Theta} - \sigma_{z\Theta})^2 + 4\tau_{\Theta z}{}^2}\right] \quad \textit{(eq.27)}$$

$$\sigma_3 = \frac{1}{2}\left[(\sigma_{\Theta\Theta} - \sigma_{z\Theta}) - \sqrt{(\sigma_{\Theta\Theta} - \sigma_{z\Theta})^2 + 4\tau_{\Theta z}{}^2}\right] \quad \textit{(eq.28)}$$

As the compressive stresses have positive sign, the highest tensile stress will be determined by the smallest negative principal stress. According to the equations given above, σ_3 causes the highest tensile stress. Considering the pore pressure P_p, the fracture initiation takes place according to the equation:

$$\sigma - P_p < T_0 \quad \textit{(eq.29)}$$

As the principal stress σ_3 is related to $\sigma_{\Theta\Theta}$ and $\sigma_{z\Theta}$, which depend on P_w, the breakdown pressure P_f can be calculated as follows:

$$P_f = 3\sigma_h - \sigma_H - P_p + T_0 \quad \textit{(eq.30)}$$

where σ_h is the minimum horizontal stress, σ_H is the maximum horizontal stress, P_p is the pore pressure (the pressure in the fracture or in the pores where the fracture is formed) and T_0 is the tensile strength of the rock. If the formation has a low porosity, no fluid can flow, so the pore pressure can be regarded as zero.

This model for the estimation of the breakdown pressure is called the “classic” or “conventional” breakdown model and it is valid foe a non-perforated vertical borehole (pre-conditions: $\Psi = 0^0$, $\beta = 90^0$, $\Theta = 0^0$).

The equation above (30) represents an upper boundary for the estimation of the initiation pressure. The lower boundary is expressed by Haimson's model ((Gou, Morgenstern, & Scott, 1993) and (Hossain, Rahman, & Rahman, 2000)):

$$P_f = \frac{3\sigma_h - \sigma_H + \sigma_1 - \alpha\frac{1-2\nu}{1-\nu}P_p}{2 - \alpha\frac{1-2\nu}{1-\nu}} \quad \textit{(eq.31)}$$

where α is Biot's coefficient and n is the Poisson's ratio. The model expressed by the equation above (31) takes Biot's poroelastic theory.

According to Schmitt et al. (1989), the effective stress given by Terzaghi ($\sigma_{eff}=\sigma-P_p$) is not accurate enough. Based on this, the modified effective stress law ($\sigma_{eff}=\sigma-\gamma P_p$, $0\leq \gamma \leq 1$) is introduced. This low has allowed to formulate another breakdown model based on poroelasticity:

$$P_f = \frac{3\sigma_h - \sigma_H + \sigma_1 - \alpha\frac{1-2\nu}{1-\nu}P_p}{1 + \gamma - \alpha\frac{1-2\nu}{1-\nu}} \quad \textit{(eq.32)}$$

where γ indicates the effective stress coefficient.

The last model to introduce is the "fracture mechanics breakdown model" (Goo, Morgenstren, & Scott, 1993); in which the fracture initiates when unstable extension starts. The breakdown equation is derived under the assumption that the stress intensity factor is equal to fracture toughness ($K_I = K_{IC}$):

$$P_f = \frac{1}{h_0(x_f,r_w) + h_a(x_f,r_w)}\left(\frac{K_{IC}}{\sqrt{r_w}} + \sigma_H f(x_f, r_w) + \sigma_h g(x_f, r_w)\right) \quad \textit{(eq.33)}$$

where x_f is the fracture length, r_w the well radius, and h_0, h_a, f, g are functions of x_f and r_w.

In some cases, the pressure drops after the fracture initiation because the wellbore pressure required to initiate a tensile fracture is greater than the least principal stress. In other cases, the fracture initiation pressure is significantly lower than the least principal stress such that the wellbore pressure slowly climbs to the value of the least principal stress after the tensile fracture initiates at the wellbore wall.

When the fracture propagates beyond the vicinity of the wellbore, the fracture propagation is dominated by the far-field stresses. The equation used to calculate the fracture propagation can be given by:

$$P_{re} = \sigma_h + T_0 \quad (eq.34)$$

Thus, the equation required to propagate the fracture can be divided, conceptually, into three parts:

1. Pressure required to keep the fracture open towards the minimum stress.
2. Pressure required to flow fluid through the fracture.
3. Pressure required to overcome the resistance at the fracture tip and thus create new fracture volume.

Or

$$P_e = P(\sigma_h) + P(flow) + P(tip) \quad (eq.35)$$

c) Presence of natural fracture in the formation

In case the formation is naturally fractured, three modes of fracture propagation in the formation may take place which are crossing, opening and dilating of the natural fracture and shear slippage of the natural fracture. When an induced fracture intersects a natural one, the horizontal differential stress and the fracture angle to the natural one are the main factors that affect the fracture behavior.

When the normal stress acting on the plane of the natural fracture is insufficient to prevent the planes from sliding against each other, shear slippage occurs. The failure analysis is derived from the linear friction law (Jaeger, Cook & Zimmerman, 2007), where the relation between the shear stress and the normal stress acting on the natural fracture plane is given as:

$$|\tau| = \tau_0 + K_f(\sigma_n - p) \quad (eq.36)$$

where τ_0 is the inherent shear strength of the natural fracture plane, τ is the shear stress, k_f is the coefficient of friction, σ_n is the normal stress acting on the natural fracture plane and p is the pore pressure. Therefore, if:

$$|\tau| > \tau_0 + K_f(\sigma_n - p) \quad (eq.37)$$

then, shear slippage occurs on the plane of the natural fracture. Using a 2D stress equation, the shear and normal stresses acting on the natural fracture plane could be obtained (Jaeger et al., 2007).

When the induced fracture intersects the natural one, its tip is blunted and the pressure at the intersection is given by:

$$P = \sigma_3 + P_\sigma \quad (eq.38)$$

where P_σ is the treatment pressure above closure stress. The criterion for shear slippage can be given by:

$$(\sigma_1 - \sigma_3) > \frac{2\tau 0 - 2P\sigma Kf}{sin2\Theta + Kf cos2\Theta - kf} \quad (eq.39)$$

And for natural fracture dilation or opening as follows:

$$P > \frac{\sigma 1 + \sigma 3}{2} + \frac{\sigma 1 - \sigma 3}{2} \cos 2\Theta \quad (eq.40)$$

σ_1 and σ_3 are the maximum and minimum in situ principal stresses respectively, and Θ is the angle of fracture relative to σ_1; the angle of counterclockwise rotation from the direction of the maximum principal stress.

The dilation occurs when:

$$P_\sigma > \frac{(\sigma 1 - \sigma 3)\,(1 - \cos 2\Theta)}{2} \quad (eq.41)$$

As the natural fracture opens, fluid leak-off will increase and the net pressure (the difference between the fracturing fluid pressure and minimum in situ stress) will increase after levelling off for a period of time.

Three modes of fracture propagation will be presented as the pressure in the natural fracture increases:

1. When the normal stress on the natural fracture is highly relative to the fracture toughness of the rock, crossing of the natural fracture will occur. In this mode, the pressure at the intersection point $P_i(t)$ at t=0 is greater than the pressure required for initiating a fracture along the original path of the advancing induced fracture. As shown in figure 15(a), crossing occurs when:

$$P_i(t) > \sigma_3 + T_{0,I} \quad (eq.42)$$

Where $T_{0,I}$ is the fracture toughness of the rock in the natural fracture face opposite the blunted induced fracture created by slurry injection.

2. Dilation of the natural fracture than propagation from the tip of the natural fracture. This occurs when the pressure at one of the tips of the natural fracture exceeds the net pressure necessary for initiating the propagation from the natural fracture tip (figure 15(b)). The fracture will extend in the direction of the natural one, and that is when:

$$P_i(t) > \sigma_n + T_{0,tip} + \Delta P_{nf} \quad \textit{(eq.43)}$$

Where $T_{0,tip}$ is the fracture toughness at the tip of the natural fracture, and ΔP_{nf} is the pressure drop in the natural fracture between the intersection point and the nearest fracture tip. In this mode, in order that the fracture is able to propagate, its toughness must sufficiently be less than the toughness at point of intersection in order to overcome the pressure drop in the natural fracture and the higher normal stress. That means, there must be a weak spot in the rock that satisfies the following criterion if the fracture propagation is to begin from the natural fracture tip; otherwise, the fracture will initiate opposite to the blunted fracture. The criterion is given by:

$$T_{0,tip} < T_{0,I} - (\sigma_n + \sigma_3) - \Delta P_{nf} \quad \textit{(eq.44)}$$

3. Dilation of the natural fracture and breakout of a fracture along the natural fracture. In this mode, the pressure somewhere in the natural fracture is sufficiently high to overcome the local fracture toughness, and the fracture breaks out the natural fracture in a place between the intersection point and the tip of the natural fracture (figure 15(c)). This fracture propagation mode occurs when local flaws in the surface of the natural fracture exist. This can be paraphrased as:

$$T_{0,1} < T_{0,I} - \Delta P_1 \quad \textit{(eq.45)}$$

Where ΔP_1 is the pressure drop in the natural fracture between the intersection point and position 1. Also, the pressure drop at the tip of the natural fracture should be lower than the pressure required to propagate the fracture at this point.

It should be noted that the expressions given above are based on idealized conditions. The real fracture pressure will depend on stress conditions, borehole direction and inclination, rock properties (tensile strength, permeability, …), borehole fluid properties and operational procedures.

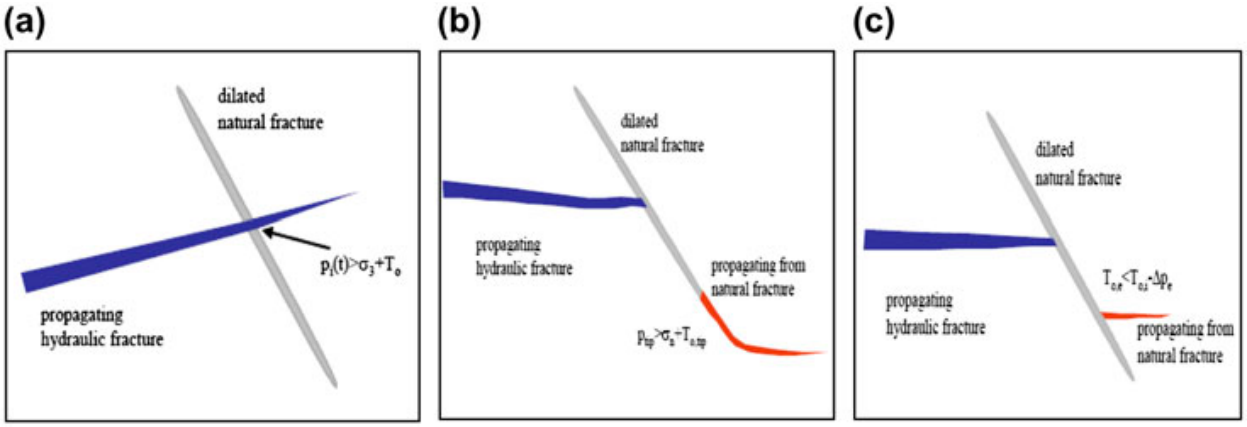

Fig. 15: Schematic illustration for induced and natural fracture interaction: (a) induced fracture crosses the natural fracture, (b) induced fracture propagates from the natural fracture tip, and (c) induced fracture propagates from weak point along natural fracture.

d) Fracture geometry

It is important to study the fracture geometry in order to design the fracture treatment. The maximum or average fracture width (aperture), borehole pressure, half-length, and height of the fracture are important values to get insight into the simulated formation processes. There are many fracturing models (Adachi et al. 2007), but the most common ones are:

- The Perkins-Kern-Nordgren (PKN)
- Khristianovic-Geertsma-de Klerk (KGD)
- Circular fracture model

i. The Perkins-Kern-Nordgren model (PKN)

This model was developed by Perkin et al. (1961) and later Nordgren (1972) who took fluid loss into account. The assumptions of this model are:

- Vertical fracture propagating in a straight line from the well,
- Restricted vertical height,
- Fracture is in plane strain in the vertical,
- Vertical cross-section has an elliptical form,
- Isotropic, homogenous, linear elastic rock mass,
- Effect of fracture toughness on geometry is negligible.

In this model, the gravitational effects are not taken into consideration. The geometry of a PKN fracture is shown in figure 16. This model assumes a constant

fracture height which is independent of the fracture length; also, a plane-strain model is assumed in the vertical plane where the fracture has an elliptical cross-section in the horizontal and vertical directions (the width is not constant along the fracture height and length). It is also assumed that the fracturing energy from the fluid injection would be consumed only by an energy loss from fluid flow (it is a viscosity dominated regime), and it ignores pressure toughness.[22]

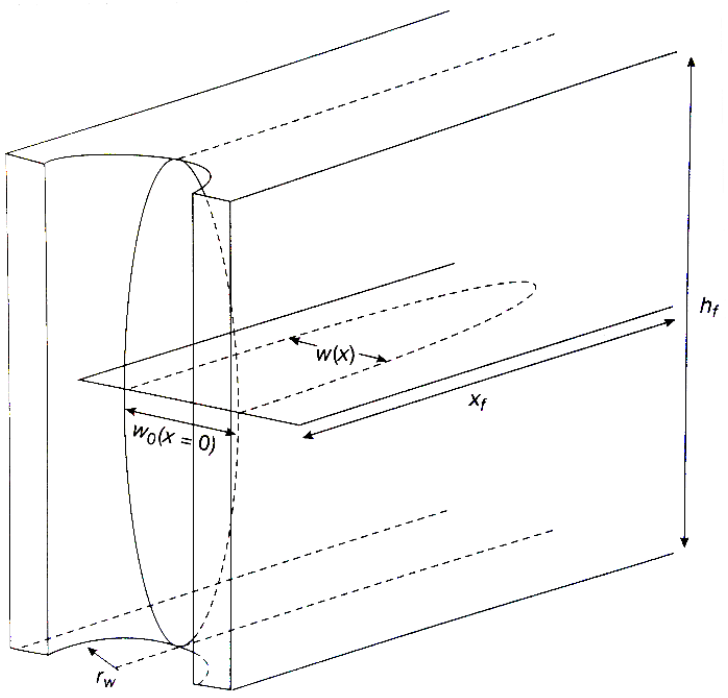

Fig. 16: Perkins-Kern-Nordgren model geometry

The fracture width is given by w and is a function of the distance x from the wellbore. w_0 is the maximum fracture width and it occurs at x=0, where a fracture wing touches the wellbore. x_f expresses the fracture half length, h_f the fracture height, and r_w the wellbore radius. The following equations are obtained for the PKN model without fluid loss:

$$x_f = 0.68\left(\frac{GQ_0^3}{(1-\nu)\mu h_f^4}\right)^{1/5} t^{4/5} \qquad (eq.46)$$

$$w_0 = 2.5\left[\frac{(1-\nu)\mu Q_0^2}{Gh_f}\right]^{1/5} t^{1/5} \qquad (eq.47)$$

$$P_w = \sigma_3 + 2.5\left[\frac{G^4 \mu Q_0^2}{(1-\mu)^4 h_f^6}\right]^{1/6} t^{1/5} \qquad (eq.48)$$

where G is the shear modulus, Q the fluid injection rate, μ the fluid viscosity and t the time. The PKN model gives good results for the stage of fracture where x_f is much larger than h_f ($x_f >> h_f$).

the length and width for the PKN case with leak-off coefficient is given below:

$$x_f = \frac{Q_0 t^{1/2}}{2\pi C h_p} \qquad (eq.49)$$

$$w_0 = 1.6\left[\frac{(1-\nu)\mu Q^2}{G C h_p}\right]^{1/4} t^{1/7} \qquad (eq.50)$$

where h_p is the height of the pay zone, and C is the total leak-off coefficient.

ii. The Khristianovic-Geertsma-de Klerk model (KGD)

The KGD model is the second model used for fracture prediction. It is developed by Geertsma et al. (1969) and is valid under the assumptions listed below:

- Vertical fracture propagating in a straight line from the well,
- Restricted fracture height,
- Homogenous, isotropic, liner elastic rock mass,
- Purely viscous fluid in laminar flow regime,
- Geometric fracture-extension patterns are simple,
- Rectangular vertical cross-section of fracture,
- Plane strain conditions in the horizontal plane,
- Barenblatt-shaped fracture tip.

A Barenblatt fracture is a cusp-shaped crack. It is only the crack contour for which the released energy by a small contour change in the vicinity of a given point is zero; this means the stress singularities of the linear elastic solution at the fracture tip are removed and equilibrium is reached only for such cracks. Figure 17 shows a sketch of the Barenblatt's contour condition for the fracture.

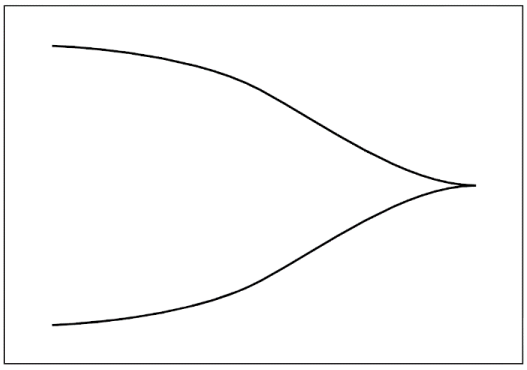

Fig. 17: Barenblatt's contour condition for the fracture tip

The KGD fracture model is shown in figure 18. This model assumes a 2D plane-strain model in a horizontal plane with a constant fracture height. An elliptical horizontal cross-section and rectangular vertical cross-section are assumed, and the fracture width is not dependent of the fracture height and is constant in the vertical direction. In the horizontal plane, the rock stiffness is also taken into consideration[22]. The Barenblatt tip condition is not shown for the sake of simplicity. The nomenclature is the same as the PKN model and the gravitational effects are also not taken into consideration.

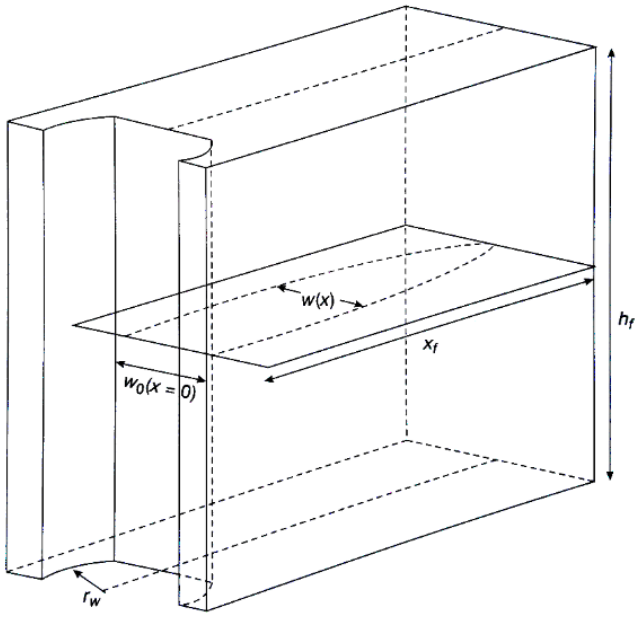

Fig. 18: The Khristianovic-Geertsma-de Klerk model geometry.

The following solutions of the KGD model can be obtained in case the fluid filled part of the fracture can be approximated by an ellipse, and the dry zone (non-fluid filled part of the fracture) in the fracture tip is small; also, in case of no leak-off.

$$X_f = 0.48\left(\frac{8GQ_0^3}{(1-\nu)\mu h_f^4}\right)^{1/6} t^{2/3} \qquad (eq.51)$$

$$w_0 = 1.32\left[\frac{8(1-\nu)\mu Q_0^3}{G}\right]^{1/6} t^{1/3} \qquad (eq.52)$$

$$P_w = \sigma_3 + 0.96\left[\frac{2G^3\mu Q_0}{(1-\nu)^3 x_f^2}\right]^{1/4} \qquad (eq.53)$$

In this model, unlike the PKN model, the wellbore pressure tends to decrease in time because of the inverse proportionality with respect to time. The KGD model gives good results for a fracture where the length of the fracture is much smaller than its height ($x_f << h_f$).

The length and width for the GDK propagation model case with leak-off coefficient are given by:

$$X_f = \frac{Qt^{1/2}}{2\pi C h_p} \qquad (eq.54)$$

$$w_0 = 0.76\left[\frac{(1-\nu)\mu Q^5}{G h_f^3 C^2 h_p^2}\right]^{1/6} t^{1/4} \qquad (eq.55)$$

another difference between the PKN and GDK models is the width-opening pressure relationship which is shown below:

$w_0 \propto \Delta px/E \rightarrow$ GDK

$w_0 \propto \Delta pH/E \rightarrow$ PKN

iii. The circular fracture model

In some cases, the minimum stress has a uniform vertical distribution which causes the shape of the fracture to be circular. The equations used for the KGD model can be transformed to obtain the relations of the circular model. The assumptions in this model are:

- Axisymmetric fracture propagation,
- Impermeable and homogenous linear elastic infinite medium,
- Newtonian fluid is injected from a point source and reaches to the tip of the crack,
- Fracture propagates continuously in mobile equilibrium,
- Lubrication theory is applicable.

The circular or penny-shaped fracture sketch is shown in figure 19 below. The approximate solutions for the fracture radius, maximum opening, and wellbore pressure are given (according to Yew & Weng, 2015):

$$R = 0.548\left(\frac{GQ_0^3}{\mu}\right)^{1/9} t^{4/9} \qquad (eq.56)$$

$$w_0 = 21\left(\frac{\mu^2 Q_0^3}{G^2}\right)^{1/9} t^{1/9} \qquad (eq.57)$$

$$P_w = \sigma_3 - \frac{5}{4\pi}\frac{Gw_0}{R} ln\left(\frac{r_w}{R}\right) \qquad (eq.58)$$

where r_w is the wellbore radius and R is the fracture radius.

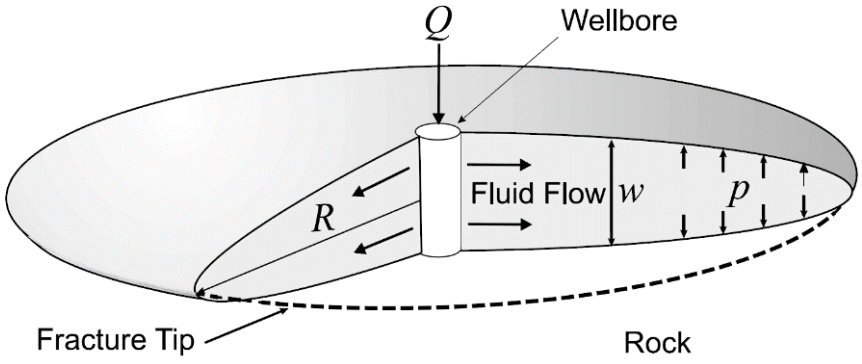

Fig. 19: Circular fracture

e) Application of the suitable model

As it is preferable to do the CRI operation in a successively layered formation of sand and shale, and as we are injecting at high depth (3000-5000 ft) and the fracture is propagating vertically, its growth will be stopped by the shale layer due to the stress variation, so the fracture length will be much greater than its height. Concerning the 2-D models used in fracture treatment designs, the PKN geometry is usually used when the fracture length is much greater than the fracture height, while the KGD geometry is used if fracture height is more than the fracture length. As a conclusion, for the study of the fracture propagation during a CRI operation, the PKN model is the most used one. The fracture is developed in two-dimensions; it is assumed that the propagation is in the vertical direction, the fracture has a constant height, and is elliptical cross-section. The fluid pressure in the fracture is assumed to be uniform over the height of the fracture. It was approximated that the plane strain prevails in planes perpendicular to the direction of propagation. However, the PKN have two limitations: (a) the plane strain approximation is true only sufficiently distant from the fracture tip and when the fracture width and pressure vary smoothly along the fracture length direction, and (b) the model application is constrained to situations where the toughness of the rock is negligible.

An advantage in using the PKN model is that a test bed could be provided for modelling the cuttings transport and fracture deflation.

By analysis of the injection portion of the data, analyzing the injection pressure allows to obtain the fracture parameters as the pressure responses during the CRI reflects the model behavior, which in this case is the PKN model. We can distinguish two types of PKN fractures: large leak-off (LL) and zero leak-off (ZL), as mentioned above. In this process, large leak-off occurs and by analysis of the data using PKN model with large leak-off (PKNLL), several parameters will be obtained; the most important ones are the fracture growth rate, or extension rate, and shear modulus of the near-wellbore formation (of the waste pod). Also, a value of closure could be obtained.

The underlying principles that are taken in case of PKNLL fracture model are given by:

- Large rate of fluid leak-off into fracture walls dominates fracture compressibility.
- Vertical extent of fracture is constant.

- Fracture elliptical in both horizontal and vertical cross sections.
- Wellbore pressure increases with $t^{1/8}$ during fracture propagation.
- Fracture length as a function of time is given by the following equation:

$$L = \frac{(\frac{q_{inj}}{2})t^{1/2}}{\pi C h} \qquad (eq.59)$$

Where L is the fracture length (m), q_{inj} is the average injection rate (m^3/s), t is time (s), C is the fluid leak-off rate ($m/s^{1/2}$), and h is fracture height (m).
The PKNLL fracture growth rate is given by:

$$PKNLLgrowthrate = \frac{q_{inj}/2}{\pi C h} \quad (m/s^{1/2}) \qquad (eq.60)$$

The PKNLL growth rate is a signification of how quickly the fracture is propagating during injection. If the value is high, that means the fracture propagation is more efficient and the CRI is more effective. Anomalously high values represent a problem because they refer to a fracture that is extending outside the specified reservoir, which could have regulatory consequences. Low values indicate that the fracture is having difficulty propagating
In order to compare the injection episodes with different injection times on the same level, the PKN length should be normalized with respect to time.
The fluid leak-off coefficient is given by:

$$1/C = 1/C_I + 1/C_{II} \qquad (eq.61)$$

$$C_I = 0.0469\sqrt{\frac{K\Delta P\phi}{\mu_{ff}}} \qquad (eq.62)$$

$$C_{II} = 0.0374\sqrt{\frac{k\phi C_f}{\mu_{rf}}} \qquad (eq.63)$$

Where k is the permeability (Darcy), ΔP is the difference between fluid pressure at the fracture face and virgin reservoir pressure (psi), φ is the reservoir porosity, μ_{ff} is the viscosity of the fracturing fluid (cP), μ_{rf} is the viscosity of the reservoir fluid (cP), and C_f is the compressibility of the reservoir fluid (psi^{-1}). C is known as the composite leak-off coefficient, which is controlled by C_I that correspond to leak-off strongly controlled by the fracturing fluid, and C_{II} that corresponds to leak-off that occurs when fracturing fluid is very similar to reservoir fluid.

The average shear modulus of the near well zone will be given by this equation, where it is calculated for each data point:

$$\Delta p = 4\left[\frac{2G^3\mu(\frac{q_{inj}}{2})^2}{\pi^3(1-\nu)^3Ch^5}\right]t^{1/8} \quad \textit{(eq.64)}$$

Where Δp is the net pressure (bottomhole pressure recorded by sensor – closure pressure, KPa), G is the shear modulus (GPa), μ is slurry viscosity (KPa.s), q_{inj} is the injection rate (m^3/s), ν is Poisson's ratio, C is the leak-off coefficient calculated above, h is the reservoir thickness (m), and t is the time since pumping begins (s). this modulus can give an idea as to whether or not the formation is becoming stiffer (higher G) as the waste pod is becoming more and more packed with slurry.

f) Fracture growth and orientation

All fractures created by slurry injection will grow in the direction of the least resistance stress, that means that the fracture will propagate normal to the smallest principal stress σ_3 in some distance from the wellbore. In a formation where the horizontal stress σ_h is represented by σ_3, at a vertical wellbore, vertical fractures will occur. Horizontal fracture can occur at depths lower than 2000 ft approximately where the overburden (vertical stress) at these depths provides the least principal stress. Once a pressure is applied to the center of the shallow formation, the fracture will open in a horizontal plane parallel to the bedding plane of the formation, because it will be easier to part the rock in this direction than in any other. At depths higher than 2000 ft, the fracture will be oriented in the vertical direction.

During fracturing, two fracture wings are generated and they extend in a σ_1-σ_2-plane (σ_v- σ_H-plane) parallel to the wellbore. it was found that the fracture orientation in the far field has a high dependency on the in-situ stress regime (Wolgast & Konietzky 2014). As an example, if a stress ratio between σ_1 and σ_3 in a stress field is close to 1, the fractures will propagate nearly in all directions; whereas, the fracture will be more linear and elongated perpendicular to σ_3 if the anisotropic character between the stresses increases. Significant anisotropy in stresses is necessary to create clear oriented fractures.

The fracture growth can be also limited by the vertical stress distribution, and variation of elastic properties. If the targeted formation is layered upward and downward, the associated stress or rearranged property of the rocks may restrict the fracture growth in height. The layers in which the fracture is not able to propagate are called barriers. It was also found that the stress contrast is the

predominant factor for limiting the height growth of the fracture. The elastic properties like Young's modulus E and Poisson ratio ν, as well as permeability k, porosity Φ, and confining stress are factors the affect the length of the fracture. Finally, in the far field, the fracture growth and orientation depend mainly on the in-situ stress regime, the orientation of the borehole within this regime, the rock properties, and the acting gravity [24].

In the figures below is given the mechanism of fracture intuition and propagation with its explanation in two cases: when the fracture is created by the slurry, and the other when the fracture is created by clean water:

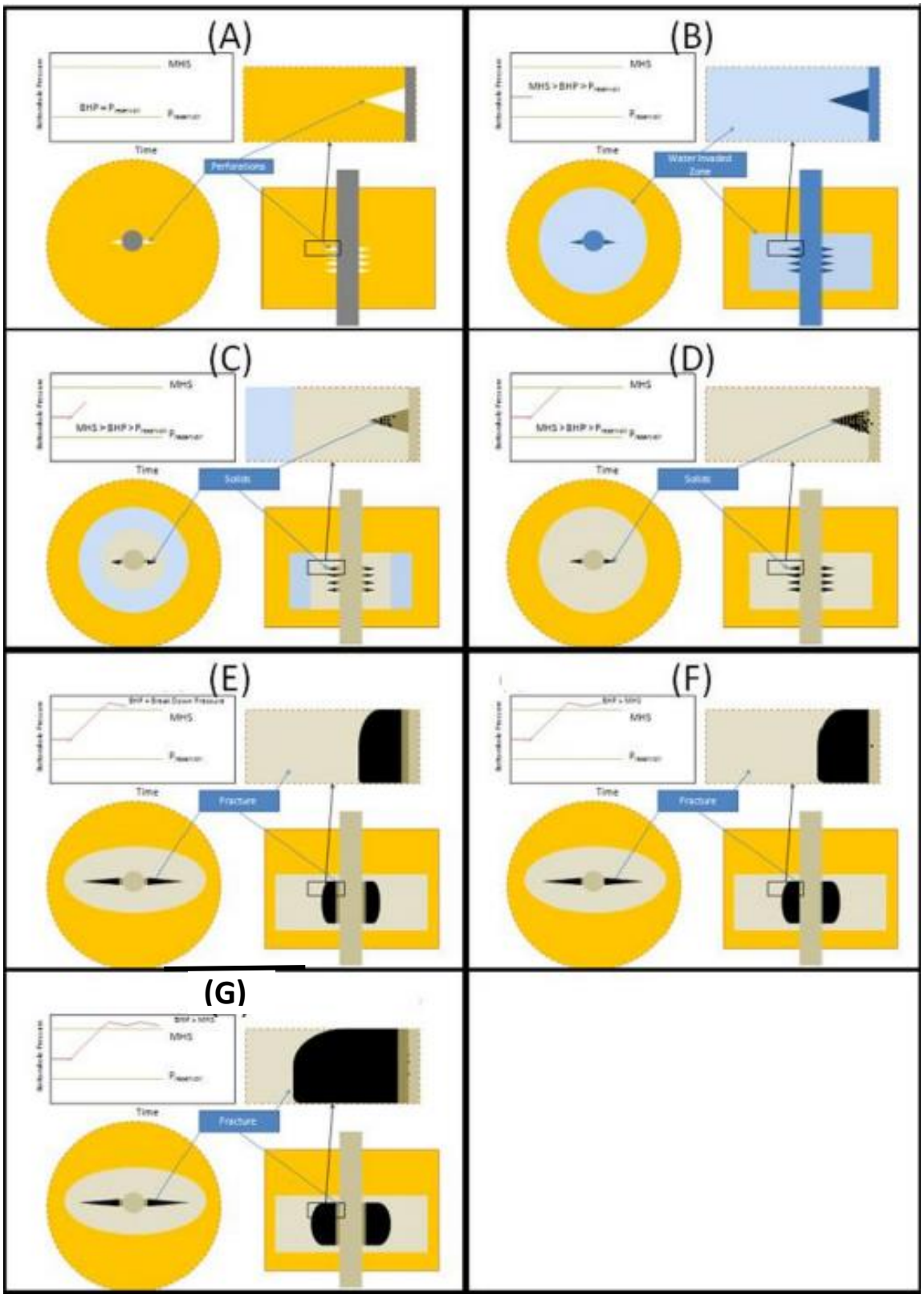

Fig. 20: Formation damage induced hydraulic fracture, (A) virgin formation; (B) matrix water injection; (C) matrix slurry injection; (D) perforation damage during slurry

injection; (E) formation breakdown; (F) fracture damage during slurry injection; (G) fraction extension during slurry injection.

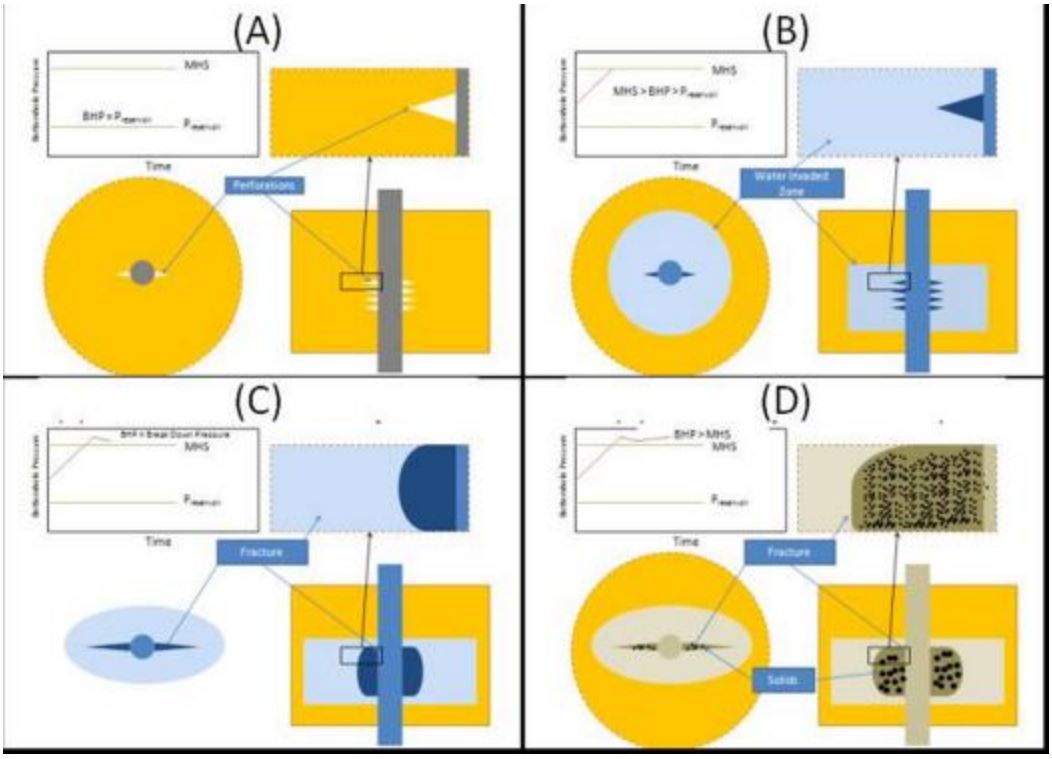

Fig. 21: Creating the hydraulic fracture with clean fluid. (A) virgin formation; (B) matrix water injection; (C) formation breakdown with water; (D) fracture injection of slurry.

Prior to any injection operation, the formation is considered to be clean, and the near-wellbore region is saturated with the formation brine (A). When clean water is injected at a flow rate lower than the fracture flow rate, water will leak off to the formation without causing a permeability damage to the near-wellbore region. The injection pressure is constant in this step (B). when the slurry is injected into the formation, a thick filter cake will be formed by the trapped solids in the perforations, and the fluid will leak off to the formation (C). solids will continue to accumulate in the perforation tunnel until the perforation is fully packed (D); this step will be accompanied with a continuous increase in the injection pressure. Once the pressure exceeds the formation breakdown pressure, a short hydraulic fracture will be created in the formation, and a slight drop in the pressure will be observed (E). proceeding with the slurry injection, more solids

will be trapped inside the fracture which will cause the injection pressure to increase again (F). with more injected slurry, solid build up in the fracture will increase the injection pressure to the point where the pressure will be high enough for the fracture to propagate to a new zone (G). the solid entrapment and the fracture propagation will continue until injection stops. To propagate the fracture, the fracture needed increases with time because more fluid pressure is lost in the fracture due to sold entrapment in the friction and increase in friction.

In figure 21, once a clean fluid is injected at high enough injection flow rate, the injection the pressure will increase as the fluids invades the formation (B). when the pressure reaches the break down point, a fracture is initiated (C). The fracture will reach the equilibrium point once the fluid leak-off rate is equal to the injection flow rate. The solids start to distribute in the pre-existing fracture once the slurry injection starts (D). In this step, the injection pressure will slightly increase as a thin filter cake, formed by the injected solids, will build on the fracture faces; that could slow down the leak-off rate [32,33].

g) Experimental observations

Laboratory tests have been applied to rock samples to study the fracture initiation and propagation inside the rock after the fluid injection. A rock, under a defined state of stress, and being injected by the slurry under a constant flow rate, will show a fracturing pressure curve as shown in figure 22 below. The black curves represent the fracturing pressures. A particular pressure-time curve could be divided into four main stages:

1. Initial pressure development stage
2. Wellbore pressurization stage
3. Fracturing stage
4. Fracture propagation stage

During the initial pressure development stage, the water is injected inside the wellbore; and its duration will depend on the time that the wellbore takes to be filled by the water. At the end of this stage, the water was just filling the pipeline and injection tube. Small pressure development is observed and the pressure curve is kept close to zero (almost horizontal) and unchanged. Continuous injection of water after the wellbore was completely filled, during the wellbore pressurization

stage, will result in the pressurization of the rock around the wellbore bottom and the quick buildup of the fracturing pressures with an almost constant increase rate.

In the fracturing stage, the fractures are initiated and propagated, new volume is created, the pressure reaches a maximum, also called breakdown pressure and then has a large drop. In this stage, fractures were continuously induced by the high fracturing pressure. After this stage, slurry injection starts. A large pressure drop is observed, and is caused by the creation of large volumes inside the fractures that will be filled by the slurry.
It was shown that the breakdown pressure increases with the increase of the injection flow rate.
The red curve represents the pressurization pressure. It helps to analyze different stages during the fracture propagation. In the initial pressure development phase, as the water only filled the injection tube and the pressure was almost kept to zero, the pressure does not change and the pressurization was kept at zero. In the wellbore pressurization phase, fracturing fluid fully fill the wellbore, and the pressure is applied to the rock mass around the wellbore bottom. As the injection flow rate is kept constant, the pressurization rate rise rapidly and then fluctuates near a constant value, this represents the ascendant of the pressure curve approximately in a straight line. When entering the fracturing phase, the pressurization rate decreases rapidly until it becomes negative, which indicates that the injection pressure decreased dramatically in a non-linear form. It showed that fractures propagated very fast, and the new pumped slurry could not fill fully the rapidly new formed ones.

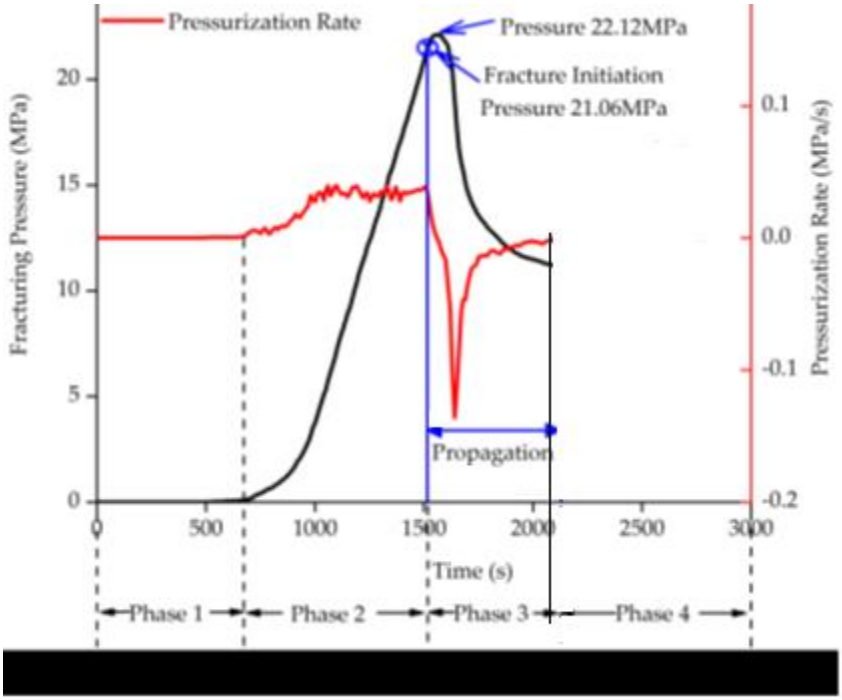

Fig. 22: The fracturing pressure-time curve and the pressurization rate-time curve

h) Fracture monitoring

Monitoring of the slurry waste injection process is accomplished through: active single-well monitoring of the injection process (injection rate and pressure, injected volume and slurry rheology); downhole monitoring (radioactive tracers, bottomhole tiltmeters, temperature survey, electromagnetic measurements); testing formation response (measurement of bottom hole pressure); and finally remote unconventional monitoring using microseismic or surface deformation (surface tiltmeters) or from adjacent wells. All these monitoring methods, except for surface and bottomhole pressure, provide limited data and are applicable for limited times. Microseismic and tiltmeters are expensive to use and are more accurate for large scales projects; with the microseismic the more accurate method to use to define the main fracture and its growth.

The opening and closure of multiple fractures can be detected from step rate tests and pressure fall-off tests. To be able to distinguish between matrix flow (when all fractures are closed), and fractured flow (when a fracture is created or becomes open), the step rate test should be analyzed based on multi-rate pressure transient method. This will allow the detection of multiple fracture opening events. An example based on multi-rate pressure transient analysis for a step rate test on a

well is given in figure 23 (using Odeh-Jones method). The trend of this curve is generally the same for every multi-fracturing process. In the plot, we distinguish three clusters which indicate multiple fractures opening process during the step rate test. The cluster at the top indicate indicates injection when all the fractures were closed. This is followed by a period of fracture growth shown by the cluster in the middle. After several injection steps, the fracture growth has stopped; then the growth of another fracture system appear as the injection rate or pressure increased. It is shown that at least three fracture system exist in this injection operation, and each fracture has a slightly different facture closure.

On the pressure fall-off test (figure 24), multiple closure events are shown (the simulation was made on the same well from figure 23). When a fracture is early in the fall-off test, pressure decline can show a one-half and/or one-quarter in the derivative slope. When fracture closure and progress occurs, subsequent peaks are observed. Multiple peaks are indications of multiple fracture closing events during the test, or different closure stresses in different zones [37,38,39,40].

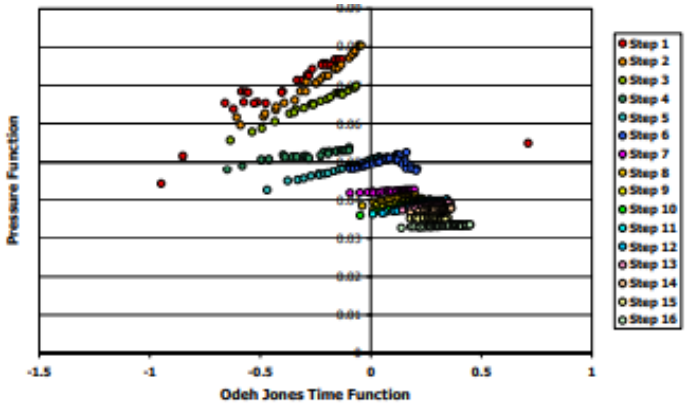

Fig. 23: Multi-rate pressure transient step rate analysis, multi-fracture initiation & propagation.

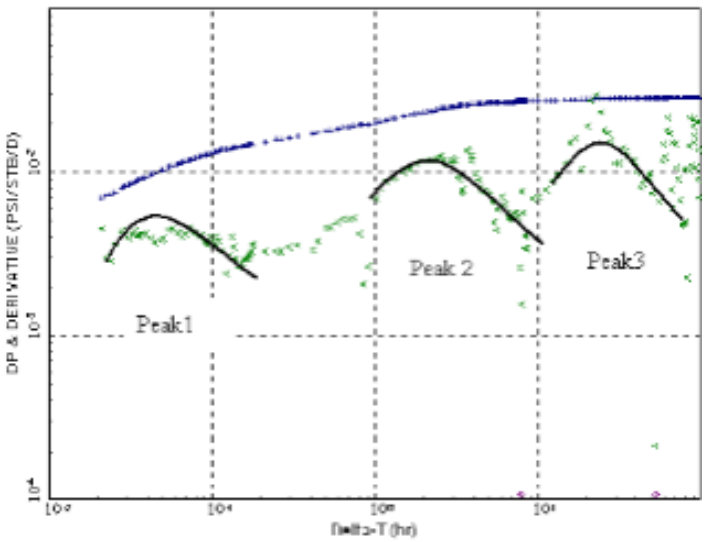

Fig. 24: Pressure and its derivative data from a pressure fall-off test

i) Vertical containment of the fracture

Fracture propagation will occur almost equally in the vertical and lateral directions. The extent that a created fracture will propagate is controlled by the upper confining zone or formation, and the volume, rate, and pressure of the fluid that is pumped. The extension will continue until either:

1. A stress barrier is encountered: a typical barrier consists of thick shale in which the minimum horizontal stress is significantly greater than that of the injection interval. Upon reaching a stress barrier, the fracture begins to expend most of its energy by propagating laterally. As the wellbore pressure is increased to compensate for the increasing frictional pressure losses in the system, or due to the clogging of the fracture tip, the fracture will extend farther more into the stress barrier.
2. A bleed-off zone is encountered: the bleed-off zone is defined as an interval with horizontal permeability greater than those of the pay zone. Upon reaching a higher permeability interval, the vertical and possibly the lateral extension of the fracture may be suspended due to pressure bleed-off. Filter cake buildup at the edge of the fracture that intersects the bleed-off zone, caused by the continuous injection operation, may effectively shut off the flow into that zone, and allow additional lateral propagation of the fracture.

3. Hydraulic horsepower limitations: in order to continue to extend a fracture, the pump engines must possess sufficient power to maintain a fracture tip pressure above the fracture propagation pressure. For that reason, the pump engines must have sufficient horsepower to overcome the energy losses of the system through frictional pressure drops in the tubulars and in the fracture, pressure losses due to leak-off into the surrounding formation matrix, and keep supplying the required energy to the system. This can impose a practical limitation on the vertical and lateral extension of the hydraulic fractures.
4. Fracture "roll over" due to stress field re-equilibrium: if neither the barriers nor the pump power requirements limit the vertical propagation of the fracture, it will begin, at some point to roll over to the horizontal. This is because the maximum principal stress will at some point begin to deviate from acting downward along the vertical axis; this is due to the decreasing weight of the overburden experienced by the fracture as it propagates vertically. In this case, it will be easier for the fracture to begin lifting the layers of rock than parting those layers. [17]

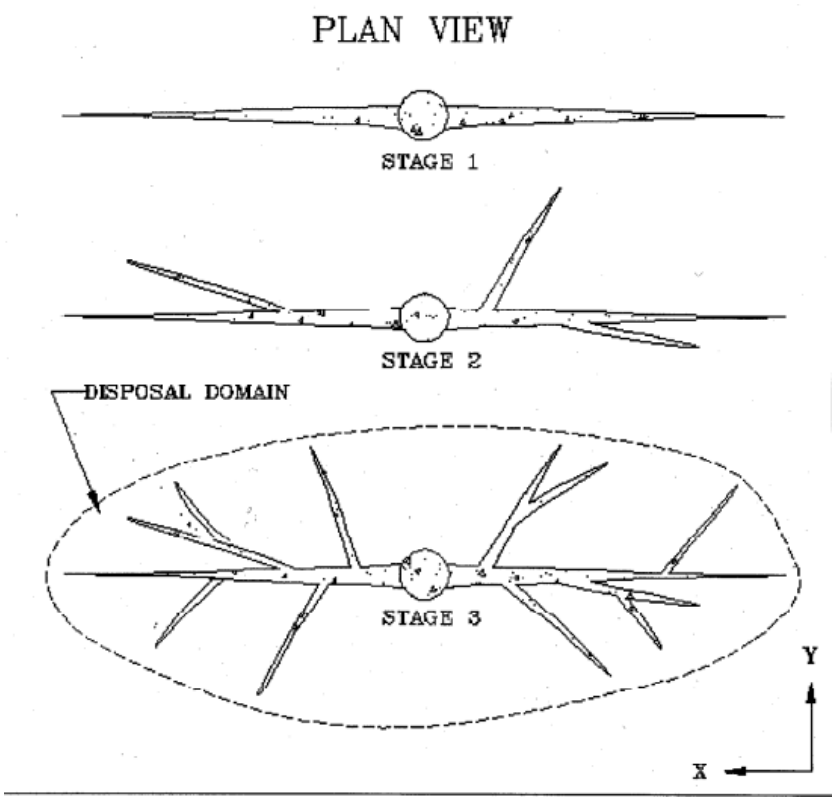

Fig. 25: Single planar fracture evolution into disposal domain

j) Fracture closure

Fracture closure is used to estimate the smallest in-situ stress (σ_3). When the fracture penetrates into the virgin formation beyond the influence zone, it will close when the fluid pressure in the fracture equals the stress acting normal to the fracture (σ_3). In most cases, the closure stress is equal to the minimum horizontal stress in the formation (σ_h).
As the closure pressure is due to the fact that fracture closure is not instantaneous, uncertainties are present in the interpretation of the minimum in-situ stress to determine the closure pressure. Fracture closure is considered to be gradual; from the moment of first physical contact between the two fracture faces, until there is no further deformation of the fracture faces. The use of tiltmeters has shown that the fracture closure process is characterized by smoothly decreasing deformation; and the minimum in-situ stress cannot be accurately determined by recording the pressure in the wellbore.

- **Shut-in/decline tests for σ_3 estimation**

When the injection operation stops and the fracture is shut-in, the pressure required for fracture opening and that required for fluid flow in the fracture will immediately drop to zero. This means that the fracture in the fracture is equal to the smallest principal stress plus whatever additional pressure left in the fracture. In case the injected slurry has a low viscosity (close to water), and the fracture is small, the additional pressure in the fracture may be small. In this case, the smallest in-situ stress is approximated to be equal to the pressure measured directly after shut-in. this pressure is called the instantaneous shut-in pressure (ISIP). This situation is shown in the figure below (figure 26): it is shown the stress where the surplus pressure has bled off and the fracture is actually closing. This is detonated as the closure pressure (P_c) and is always the best estimate of σ_3.

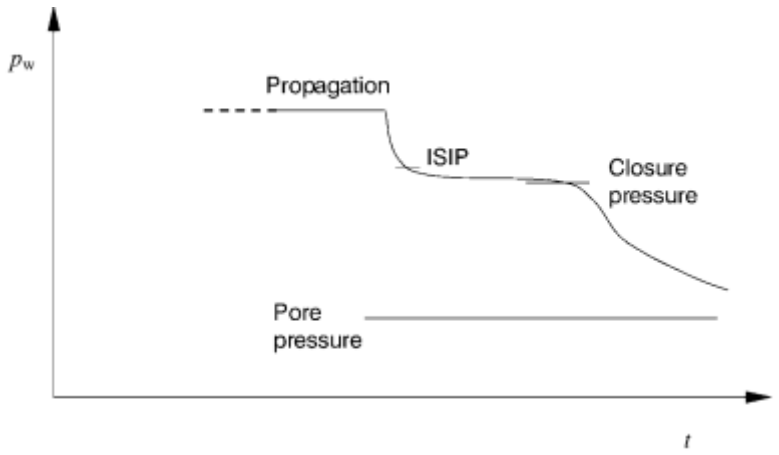

Fig. 26: Well pressure response after shut-in

However, the best estimate of σ_3 is obtained by waiting until the fracture closes, because the ISIP may be significantly higher than the closure pressure depending on several factors like fluid viscosity, leak-off into the formation, and pump rates. Thus, the ISIP is always considered to be an upper bound to σ_3 value, but the difference between the shut-in pressure and σ_3 value may be significant, and varies from a test to another. Since fracture closure happens gradually rather than instantly, accurate identification of the closure pressure may not be easy. When physical contact between the two fracture faces is established, the fluid in the fracture may still be free to flow. The two fracture faces may also have been distorted relative to each other. For the ideal case of instant closure, there should be a distinct change in the response, indicating the start of rapid pressure drop. This is caused by the sharp increase of the system stiffness as the fracture closes. The real response will depend on the nature of the slurry, the permeability of the rock and the stiffness of the system.

To assist in the interpretation of fracture pressure response, two plotting methods are mostly used: the derivative plot method and well test analysis.
In the derivative plot method, where the rate of pressure decline (dP/dt) is plotted against bottomhole pressure, the ISIP occurs at the pressure where the most negative dp/dt occurs. Closure is determined at the point where dP/dt points deviate from a straight line as shown in figure 27.

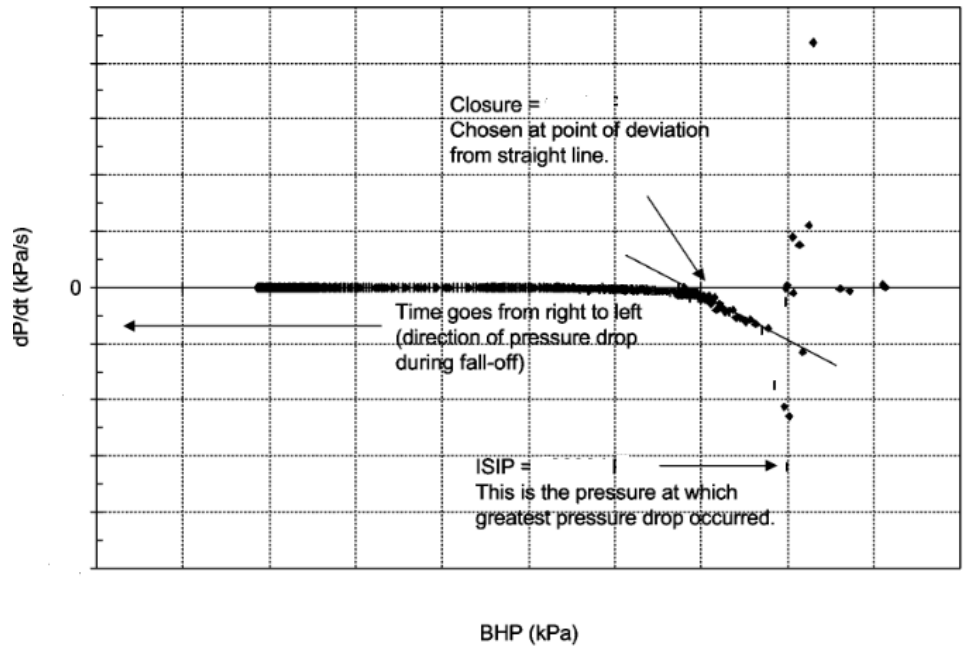

Fig. 27: ISIP and closure pressure on the pressure derivative plot

The other technique in determining the ISIP and closure pressure is from well test analysis. In this case, ISIP will be defined as the first point at which wellbore storage is observed. Closure pressure is determined from the point at which linear flow from the fracture into the formation ceases.

Assumptions say that the cuttings are distributed uniformly across the fracture aperture and that the slip between the cuttings and the carrying fluid is only due to gravitational settling. But in reality, the cuttings tend to migrate transversely away from the fracture walls and accumulate at the fracture center, where shear stress is the lowest and flow velocity is the highest. The fracture geometry and the distribution of the encased cuttings condition the closure behavior of the fracture.

IV. FLOW RATE STUDY AND SLURRY RHEOLOGY

1. Injection flow rate determination

The main goal of a CRI operation is to get rid of the drilling waste by injecting a slurry with high solid content (up to 40%) into the target formation, in the most environmental way. This is accomplished by injecting first a pad of clean fluid to open the fracture to prevent the plugging of the near-wellbore pore space. Once the fracture is created, the slurry will be introduced to the formation. If the formation has a high permeability-thickness product (k x H), a high injection flow rate is needed to open up the fracture with clean fluids.
If the slurry is injected at a flow rate which is insufficient to open the fracture due a lack of geomechanical understanding with the combination of poor injection or facility design, a high formation damage around the wellbore will be created. When the slurry is injected under a matrix flow regime, suspended solids will plug the near-wellbore pore throats and will form a filter cake layer at the face of the formation, which will increase the injection pressure. When the injection pressure exceeds the formation fracture pressure, the formation will finally fracture. But the presence of the filter cake in the near-wellbore will cause problems in the future injection and leak-off characteristics. In addition, the damage will cause the injection pressure to buildup rapidly, facilitating the creation of short fractures that causes the near-wellbore stresses to increase more rapidly for a certain amount of solid deposition than in the case with longer fractures.

In order to create a fracture, the pressure in the wellbore must be increased by pumping the fluid in the wellbore at high rate. When the pressure reaches a value bigger than the breakdown pressure of the formation, fracture will initiate. The breakdown pressure is the sum of the in-situ stress and the tensile strength of the rock. When the fracture is created, it extends using the fracture propagation pressure, which is equal to the sum of the (a) the in-situ stress, (b) the net pressure drop, and (c) the near-wellbore pressure drop. The net pressure drop is equal to the pressure drop down the fracture as a result of the viscous fluid flow in the fracture, in addition to any pressure increase caused by tip effects. The near-wellbore pressure drop is a combination of the pressure drop of the viscous fluid flowing through the perforations, and the pressure drop resulting from tortuosity between the wellbore and the propagating fracture. Accordingly, the slurry properties are very important in the creation and propagation of the fracture.

A study was made on three waste disposal wells in three different high permeability sandstone formations in order to evaluate the effect of hydraulic fracturing on the well longevity and to define the right injection flow rate to also maintain the longevity of the well.

	Well 1	Well 2	Well 3
Well type	Commercial disposal well for oil & gas	Bio-waste injector	Commercial disposal well
Formation type	Sandstone	Sandstone	Sandstone
Permeability (mD)	350-3500	300-500	50-100
Porosity	0.25	0.26	0.17
Thickness (ft)	120	262	180
Total Formation compressibility (psi^{-1})	$6.5x10^{-6}$	$6x10^{-6}$	$3.6x10^{-6}$
Formation pressure (psi/ft)	0.445	0.445	0.4
Formation top depth (ft)	5600	4790	6400

Table 3: wells geological properties

A step rate test was conducted to define the formation fracture pressure and the critical flow rate prior to injection. Clean water (0% solids) was used in the 3 wells.

Ideally a step rate test is run to identify the fracture injection flow rate. But in some cases, due to poor design of the step rate test, the flow rate will be too low and the fracture initiation point cannot be identified as shown for well 1. In this case, an alternative method is used to calculate the fracture flow rate by using the diffusivity equation to calculate the injection pressure at constant injection flow rate:

$$\text{BHP} = \frac{162.6Q\beta\mu}{kh}\left[log\left(\frac{kt}{\phi\mu C_t r_w^2}\right) - 3.23 + 0.87s\right] + P_i \qquad \textit{(eq.65)}$$

Where:

β = the fluid formation volume factor,
μ = the fluid viscosity,
k = the formation permeability,

h = the formation thickness,
t = injection duration,
φ = formation porosity,
c_t = total compressibility,
r_w = wellbore radius,
S = skin factor,
P_i = initial reservoir pressure.
The formation fracture pressure can be identified by using wireline logs.
This equation was used in the 3 wells in order to calculate the flow rate.

In the table below are shown the injection history of each well, along with the number of injection steps and the rate range.

	Well 1	Well 2	Well 3
Number of injection steps	5	4	6
Flow rates range (bbl/min)	2-7	3-9	2-14
Batch volume injected (bbl)	100-3000	8000-10000	5000-10000
Solids percentage in slurry	10-23%	10-12%	5-12%
Injection duration (days)	1490	760	790

Table 4: injection history of the 3 wells.

- **Interpretations**

For well 1: from the results shown on a pressure-rate plot, we see two lines with the same exact slope, that indicates matrix flow and no fracture flow was captured. The presence of two lines is related to the fact that the first three steps (2, 3 and 4 bbl/min) were too short to allow the pressure to stabilize, while the two last steps were long enough to show formation behavior.

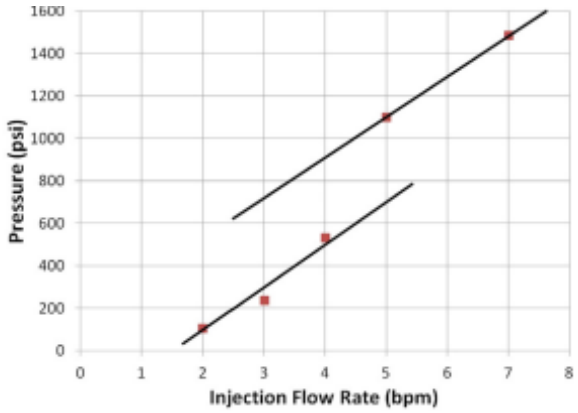

Fig. 28: step rate test analysis

Figure 28 represent the injection pressure vs. injection flow rate calculation for the studied well. It is shown that an injection flow rate higher than 10 bbl/min is needed to initiate the hydraulic fracture without damaging the formation. In addition, the injection flow rate should remain lower than 20 bbl/min to avoid breaking down the containment layer. The fracture pressure increases with the increase of the flow rate due to higher friction loss in the well tubing (the pressure data plotted is calculated at the wellhead).

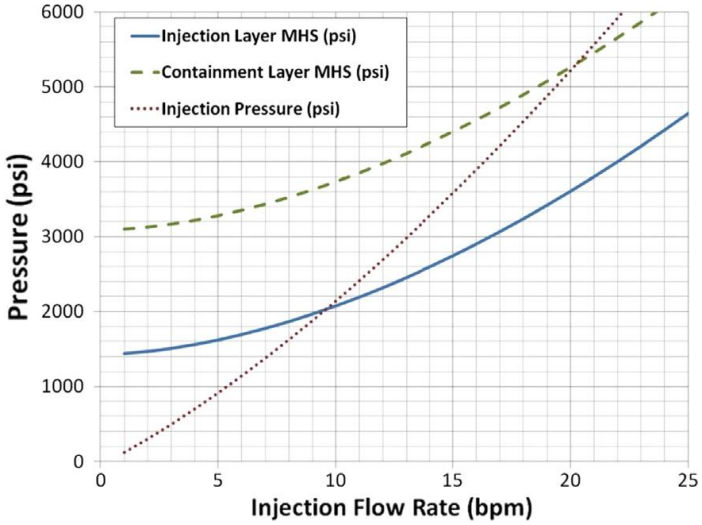

Fig. 29: Injection pressure calculation for well 1

The disposal started at an injection flow rate between 4 and 5 bbl/min, which is lower than the formation critical flow rate obtained from the step rate test, and injection pressure of 1000 psi. Over time, a serious injectivity loss took place, with

a linear decline in the injection flow rate in order to maintain the injection pressure at 1000 psi

Despite the continuous drop in the injection flow rate, it was not possible to maintain the pump pressure at a constant value (1000 psi) so a linear increase in the injection pressure was observed. The injection pressure has increased to 1600 psi, as more slurry is being injected, in less than a year as more internal and external filter cake had built up around the wellbore. After 4 years of operation, the well became completely plugged and the injection operation was aborted.

Two fracture simulation cases were conducted for well 1 by using a commercial fracture simulation software (@FRAC3D). assuming two injection flow rates of 5 bbl/min: the actual field injection flow rate, and 15 bbl/min: injection flow rate higher than the calculated fracture flow rate; at 5 bbl/min, the fluid is leaking off the fracture rapidly, which will result in a short and solid packed hydraulic fracture. At 15 bbl/min, a longer fracture will be created with much lower solid concentration inside the fracture. The results are shown in figure 30.

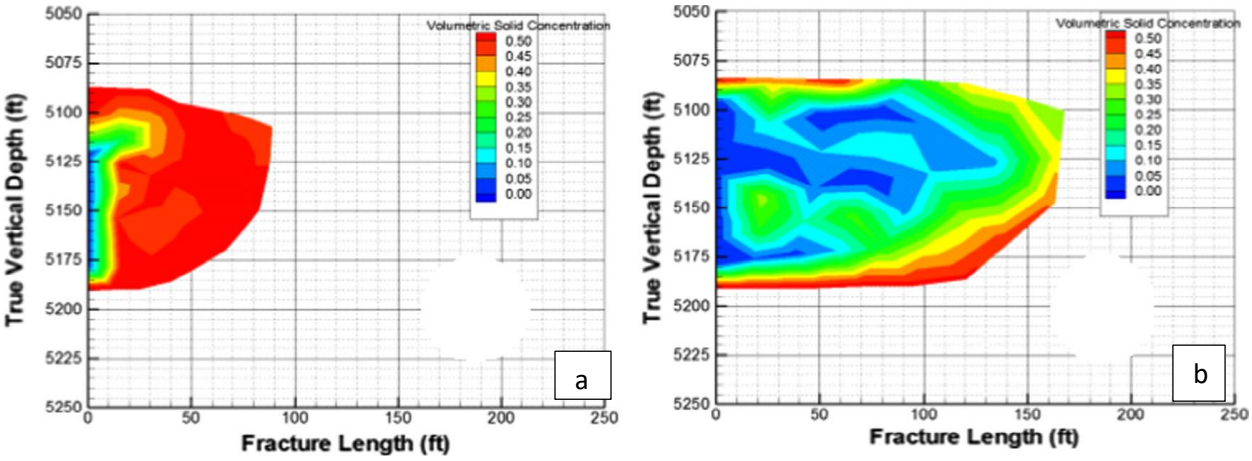

Fig. 30: Fracture simulation results for well 1. (a) Q=5bbl/min, (b) Q=15bbl/min

For well 2: On the pressure-rate plot, we see only a linear line which means there is no transition from matrix to fracture flow and higher injection rate is needed in order to fracture the formation with clean water.

The injection was conducted at an injection flow rate higher than 23 bbl/min in order to create a hydraulic fracture.

The injection rates at which the operation started were lower than the formation fracture flow rate obtained from the step rate test. The injection pressure was stable

and ranged between 2750 and 3000 psi. although the injection pressure was stable during the well life, the shut-in pressure fall-off rate declined with time because of the organic solid build up in the near-wellbore region. A higher injection rate in the well, or the nature of the wastes injected in the well could cause this change in the well behavior.

As a conclusion, by simulating the fracture in well 2, it was shown that at an injection flow of 10 bbl/min, which is lower than the fracture flow rate, a short and solid packed hydraulic fracture is created. While at an injection flow rate higher than the fracture flow rate is applied (25 bbl/min), a longer fracture is created with much lower solid concentration inside the fracture. This is shown in figure 31.

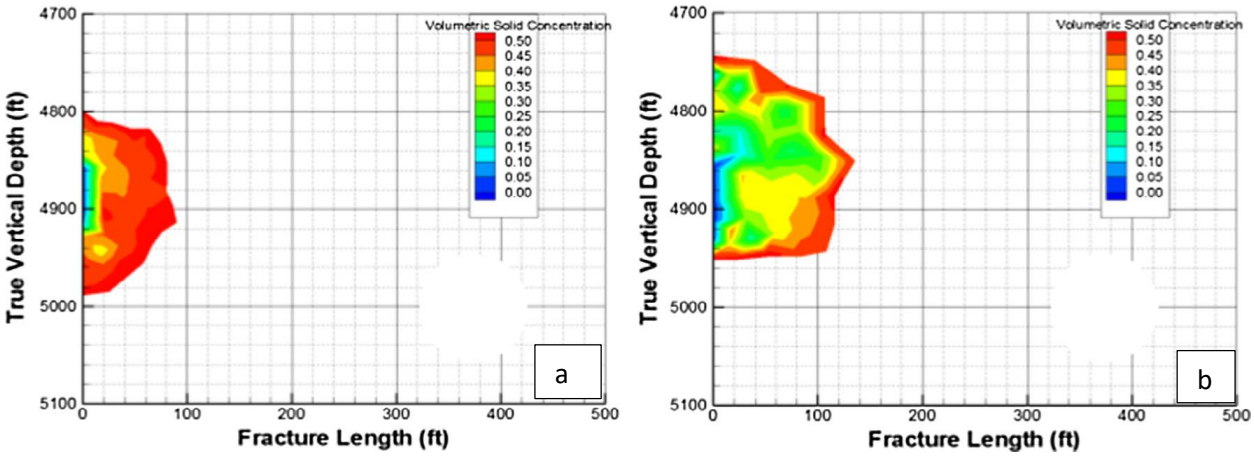

Fig. 31: Fracture simulation results from well 2. (a) Q=10bbl/min, (b) Q=25 bbl/min

Well 3

For well 3: In the pressure-rate plot given in figure 32 shows that the transition from matrix to fracture injection has occurred at a flow rate of 4.5 bbl/min, and a pressure of 1370 psi.

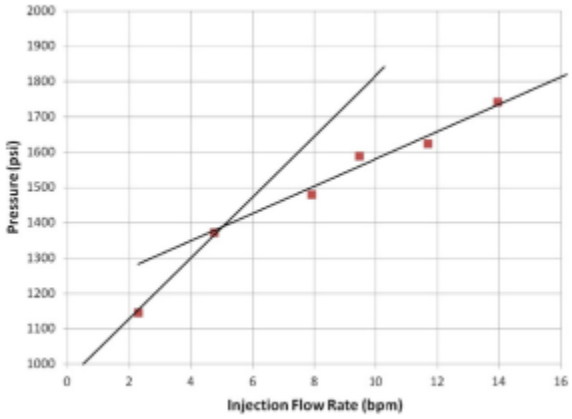

Fig. 32: Step rate test analysis in well 3

The injection flow rate used in this operation is higher than the formation fracture flow rate given by the step rate test. The pressure history shows cycles of increasing pressure plus damage build up inside the fracture, followed by a decrease in pressure associated with pressure propagation and/or opening up new fractures.
The fractures formed in this well have a low solid concentration as the injection was conducted at injection flow rate (10bbl/min), higher than the fracture flow rate.

- **As a conclusion** from the study above, we see that by injecting the slurry at a flow rate lower than the fracture flow rate, the fracture will plug quickly, which will shorten the formation ultimate capacity to store solids. Also, a high solid concentration will block the fracture faces and will reduce the leak-off rate and increase the injection pressure.

Selecting the right injection flow rate is considered to be a critical step in designing a cuttings re-injection operation. Using the correct flow rate will prevent the damage of the near-wellbore region to create a fracture that risks in plugging the formation and result in a significant increase in the injection pressure over a short time. This will impact the formation storage capacity and will shorten the life of the injection well.

2. Slurry rheology

The slurry is made up of solid parts (cuttings), liquids (water, mud) and possible chemical additives.

As a good fracturing fluid, the injected slurry should have these main objectives:

- allow the initiation of the formation breakdown and propagation through the formation.
- Facilitate cuttings transport by allowing them to flow into the created fractures to keep a sufficient area open in the fracture.
- Minimize fluid leak-off into the formation. If an excessive amount of fluid leaks into the formation, the transport of the cuttings and the propagation of the fracture will not be accomplished.

Slurry should be designed in a way to provide sufficient solids carrying capacity to hold the cuttings in suspension in surface tanks and in static conditions, and to eliminate the risk of surface lines and equipment plugging. Also slurry should be designed with an optimized rheological properties and particle size distribution to prevent premature settling nearby the disposal zone, in order to extend the life of the available annulus and maximize its utilization.

The different flow characteristics of each component contained in the slurry can be best described in terms of viscosity. Using a viscometer to directly measure the slurry viscosity is never attempted; the viscosity should be calculated based on the pressure drop in the pipeline leading to the wellhead and in the well tubing.

a) Solids present in the slurry

Solids are considered to be the most important and variable components of the slurry; for full characterization, it is necessary to know the quantity present, the size, and finally the lithology, including the approximate shape of the particles, their chemical composition and expected behavior. The behavior of the slurry, as well as the minimum speed required to have solid suspension, the type of motion, and many other aspects are highly influenced by the size of the particles constituting the slurry and their concentrations. These two parameters should be determined to be able to study thoroughly the problem from the point of view of design of the machine that should be able to provide the required pressure Generally, the solid percentage un the slurry should be between 10-20%, it is an acceptable choice from the point of view of the plant design. Higher concentration

of solids in the slurry require a more complex study on the transport and flow. In reality, the solids concentration in the slurry can be as high as 30 to 40 percent by volume for fine grained material (less than 150 μm), and on the order of 10-20 percent for coarser materials (150-300 μm).
The size of the particle depends on the degree of crushing. All the solids of a cuttings re-injection process generally have a size of the order of a few hundred micrometers. The particle size ranges between 2-300 microns. As study show, more than 90% of the analyzed particles has a diameter size lower than 300 microns.
Some methods are used to determine the particle size. One of these methods is the laser diffraction. It is a favored technique that is considered to be accurate and reliable. Its main advantages are that it is very flexible and can measure all types of particles, it is very rapid (results can be given in less than sixty seconds), also large numbers of particles can be sampled in each measurement. Laser diffraction measures particle size distributions by measuring the angular variation in intensity of light scattered as a laser beam passes through a dispersed particulate sample. The particle size is reported as a volume equivalent sphere diameter.[27]

b) Problems related to the use of slurry

In static conditions, the solids present in the slurry risk to precipitate over time. The settling velocity is a function of density, particle size and viscosity. A thorough study should be made to prevent this phenomenon. Solids transport models are often used to predict the minimum speed required to have the solids dragged, and the maximum time for which it is possible to leave the slurry at rest. The separation of the solid phase from the liquid phase with or without precipitation of solids at the bottom is considered to be a very dangerous phenomenon that could lead to the blocking of the system. This is called syneresis. To prevent this from happening, an amount of polymers is added is added to the compound. Another phenomenon that happens to the slurry is the sagging; it is a stratifying of the components due to their different densities; it could occur under both static and dynamic conditions and it is mostly dangerous in an inclined well of 45^0. Also, blockage of the pipeline could be caused by the slurry when it deposits and forms a barrier to the flow.

c) Slurry Composition

A slurry is mainly composed of water (about 75-90%) additives percentage is about 0.5% and the remaining is the wastes (9.5-24.5%). It is mainly composed of mudstone, sandstone drill cuttings, bentonite, fresh water and xanthan gum along with other additives.

The main slurry component is the water. First, a quality controlled should be made and the water should be filtered to 50 microns. Normally fresh water is used: seawater; but the presence of sulfate in it represent a disadvantage because it interacts with connate reservoir water and forms sulfate scales, and it provides a sulfur source for sulfate reducing bacteria.

The second main component is the cuttings waste. These cuttings are first treated to remove the coating of the drilling fluid. 100% treatment is not fully reached and some liquid remnants stay on the cuttings but in small concentrations because these remnants could have negative effects on the slurry composition and the fracturing process (for example that presence of oil at a higher concentration as mentioned before).

The main additives that should be mixed with the water and the cuttings are the following:

Clay control agents: KCl or organic clay stabilizer is added to the fracturing fluid to prevent the interaction between the water and the minerals in the reservoir. Its concentration that should be added depend on laboratory tests made (generally between 2-8% in concentration). KCl has a great ability to stabilize clays and is much more effective than other inorganic salts such as NaCl, $CaCl_2$, …

Friction reducers are added to the water to reduce the friction generated while pumping the fluid down the well tubulars. These materials are added to the fluid at a concentration of 0.25 to 2 gal/1000 gal. several forms of friction reducers could be used and are shown in figure 33 along with a comparison of friction pressure for two water mixtures.

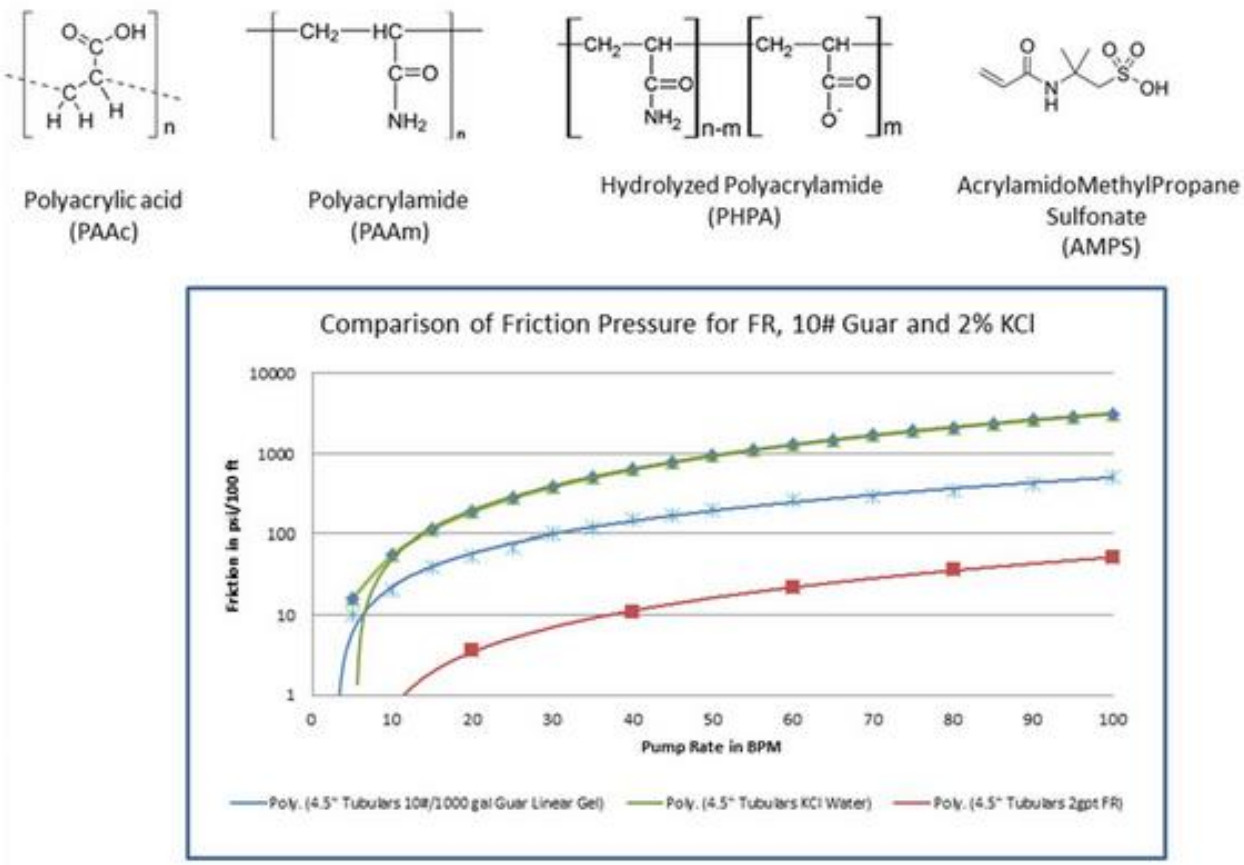

Fig. 33: Comparison of friction pressure for water containing only 2% KCl vs. water containing 2% KVl and 2 gallons per 1000 gallons (FR) and 10# Guar.

Gelling agents are added to the slurry to increase its viscosity. It increases the fracture width so it can accept higher concentrations of cuttings, improves fluid efficiency by reducing fluid loss, improves the transport of the cuttings and reduces the friction pressure. The molecular weight of the gelling agent controls its viscosity; which increases with increasing chain length and concentration. The gelling agent concentration ranges around two values known as the critical overlap concentration (C*), and the critical entanglement concentration (C**). Depending on the slurry mixture. If the concentration exceeds C**, the sineresis phenomenon will take place where the gel will be cross linked and the water will be squeezed out of the gel matrix (figure 34).

The most common gelling agents used in the CRI process are the Guar and its derivatives (HydroxyPropyl Guar, CarboxyMethyl Guar and CarboxyMethylHydroxyPropyl Guar). They could be of natural or synthetic origins.

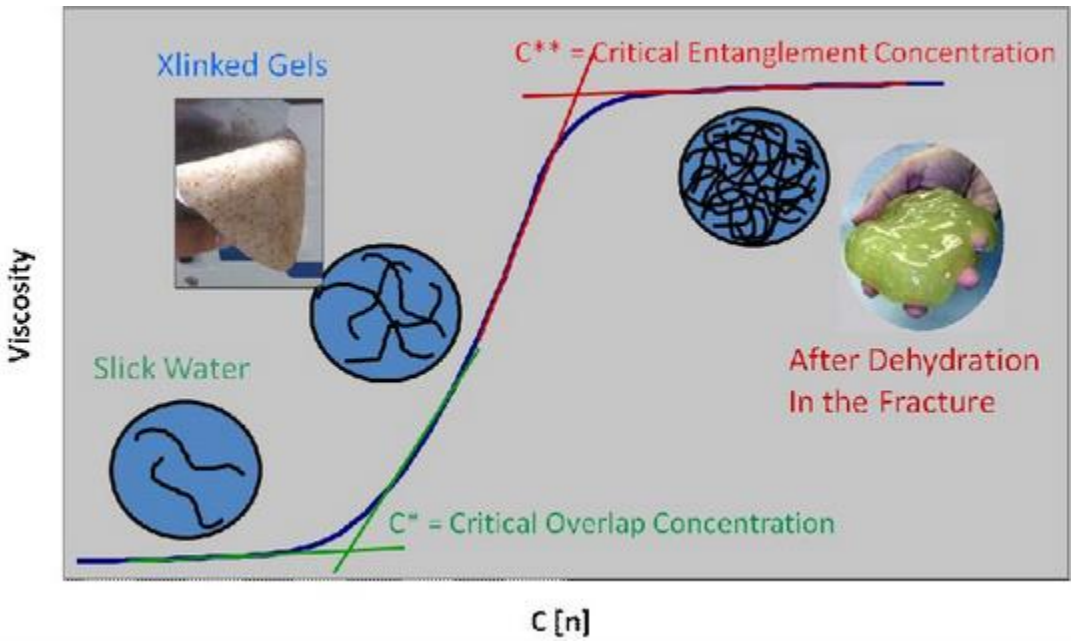

Fig. 34: Intrinsic viscosity of a solution as a function of the polymer concentration

Crosslinkers are used to increase the molecular weight of the polymer by crosslinking its backbone into a 3D structure. This could increase the base viscosity of the linear gel to 2-20 times the original value. The crosslinking can also increase the elasticity and the cuttings transport capability of the carrying fluid.

Borate in the form of Boric acid is the most common crosslinker used today. Crosslinking is a function of the pH, that means it can be formed or reversed by simple adjustment of the pH. When Borate is used, the base polymer should be mixed with a water solution having a pH=7 then adjusted to 6 to add the Borate; and during pumping, a buffer (a solution usually containing an acid and a base, or a salt, that tends to maintain a constant hydrogen ion concentration) is added to bring the pH above 8 so the crosslink could be formed.

Biocides/Bactericides are used to minimize the enzymatic attack of polymers used to gel the slurry by aerobic bacteria present in the base water. Microorganisms growth quickly degrades the polymer function. They are also added to prevent the introduction of anaerobic sulfate reducing bacteria (SRB) into the reservoir that could sour the well and produce corrosive hydrogen sulfide gas. A disinfectant could be a chemical compound (quaternary amines, amides, aldehydes and chlorine dioxide) or an ultraviolet light. A good bactericide should also inactivate the enzymes that the bacteria release. The use of a variety of

bactericides is necessary because bacteria mutate so it becomes resistant to a particular bactericide if it is continuously used.

Some example of the added compounds with their roles:

- Acids: helps dissolve minerals and initiate fissure in rock.
- Sodium chloride: allows a delayed breakdown of the gel polymer chains.
- Polyacrylamide: minimizes the friction between fluid and pipe.
- Ethylene glycol: prevents scale deposits in the pipe.
- Borate salts: maintains fluid viscosity as temperature increases.
- Glutaraldehyde: eliminates bacteria in the water.
- Guar Gum: thickens the water to suspend the cuttings.
- Citric acids: prevents precipitation of metal oxides.
- Isopropanol: used to increase viscosity of the slurry

It should be noted that for annulus injection, more additives may be needed to achieve a desired slurry viscosity to avoid solid particle settling and plugging of the annulus.

According to federal regulations, all these additives should be environmentally friendly and should be added in quantities that will not affect the water resources or the formation itself. Several of the added chemicals must be taken care with if handled at their full concentrations, but using them to manufacture the fracturing slurry, their concentrations are very dilute and pose very low hazards [28,33].

d) Viscosity

Viscosity is a very important parameter that should be studied in the slurry because its value affects the fracture width: higher viscosity will create wider fractures that can accept more cuttings; it can also reduce the fluid loss to improve fluid efficiency, improve cuttings transport and reduce the friction pressure.

Viscosity is the resistance of a fluid to a change in shape, or movement of neighboring portions relative to one another. It denotes opposition to flow. Viscosity could be taken as internal friction between the molecules; this friction opposes to the development of velocity differences within a fluid. Viscosity is considered to be an important parameter in determining the forces that must be overcome when fluids are transported in pipelines. Viscosity is the material

property which relates the viscous stresses in a material to the rate of change of a deformation (the strain rate). It could be defined in a simple shearing flow:

Let us consider a fluid that is trapped between two infinitely large plates, one fixed and one in parallel motion at constant speed u. if the speed of the top plate is low enough, then in steady state the fluid particles move parallel to it, and their speed ranges from 0 at the bottom to u at the top (figure 35). Each layer of the fluid has a higher velocity than the layer below it, and a force resisting their relative motion will be created by the friction between the layers. The fluid will apply on the top plate a force in the direction opposite to the motion, and an equal but opposite one on the bottom plate; so an external force should be applied to keep the plate movement at constant speed. The magnitude F of the force is found to be proportional to the speed u and the area A of each plate, and inversely proportional to their separation y:

$$F = \mu A \frac{u}{y} \qquad (eq.66)$$

The proportionality factor μ is known as the dynamic viscosity and it unit is Pa.s. The ratio u/y is the rate of shear deformation or shear velocity, and is the derivative of the fluid speed in the direction perpendicular to the plates. If the velocity does not vary linearly with y, the appropriate equation will be:

$$\tau = \mu \frac{\partial u}{\partial y} \qquad (eq.67)$$

where $\tau = F/A$ is the shear stress, and $\frac{\partial u}{\partial y}$ is the local shear velocity. This expression is known as Newton's law of viscosity; and each fluid exhibiting this behavior is called Newtonian fluid.

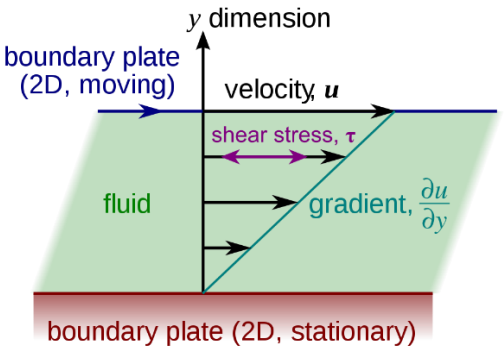

Fig. 35: Speed distribution scheme for a fluid between two slabs, one at rest and one in movement

It is sometimes more convenient to work with the kinematic viscosity (also called momentum diffusivity), and defined as the ratio of the viscosity μ to the density ρ of the fluid; its unit is (length)^2/time, it could also be stokes (British system) which is equal to one centimeter squared per second [,29,30,31]:

$$\upsilon = \frac{\mu}{\rho} \qquad (eq.68)$$

The slurry density in a CRI plant ranges between 1.1-1.4 g/cc (1100-1400 kg/m^3). The density of the slurry is given by: $\rho=(1-\varphi)\rho^f + \varphi\rho^p$. where φ is the volume fraction of the particles, ρ^p is the particle mass density, and ρ^f is the fluid density which is calculated as a mixture of the water with the additives and other waste remnant. The mixture consisting of the liquid phase will have a density based on the average weight of those of water, oil (which viscosity could be considered equal to 900 kg/m^3), and the additives. It is calculated by multiplying the density of each component multiplied by the volume fraction of each one. As for the solid phase, an approximate value could characterize the type of geology in which the cuttings come from, and it can vary between 1500 and 2000 kg/m^3. An average value equal to 1752 kg/m^3 could be considered. The contribution of the additives to the density is small considering their small volume fraction. Experiments have shown that slurry with lower density tends to lead to earlier formation breakdown, while it is quite preferable for fracture propagation

Viscosity measurement

i. Marsh-funnel

Viscosity is usually measured with a Marsh funnel. The test consists of filling the funnel with a slurry sample and measuring the time required for 1 quart (1500 mL) of the sample to flow from the initially full funnel into the mud cup (beaker); the funnel viscosity unit is seconds per quart. For example, fresh water at 75^{0}F has a funnel viscosity of 26 s/qt. Also this method is sometimes used, but it does not give exact values for non-Newtonian fluids that exhibit different apparent viscosities at different flow rates for a given tube size; that is because the flow rate from the Marsh funnel changes during measurements due to the change in the fluid level in the funnel.

The Marsh Funnel is designed so that 1500 mL of fluid can be poured into the funnel. The height of the cone-portion of the funnel is 12 in. (30.5 cm), and the diameter is 6 in. (15.2 cm). The copper tubing is 2 in. (5.08 cm) in length and has a

diameter of 3/16 in. (0.48 cm). when the fluid is poured, a small stopper is placed in the orifice at the bottom to prevent flow out while the fluid is poured into the funnel. Once the funnel is filled, the beaker is placed on a scale positioned below the funnel. The scale is connected to a computer that records weight versus time at intervals of 1 second. The weight is converted to a volume using the fluids density. For fluids with yield stress, a steady-state height is observed remaining in the funnel and recorded.
This tool is effectively practical because it takes a short operating time and can be utilized to frequently measure the funnel viscosity.
Empirical models have been developed to determine rheological parameters of the fluid using Marsh funnels. Some of them monitor the change in the fluid height in Marsh funnel with time and correlate it with the fluid rheological properties such as the plastic viscosity, yield point, apparent viscosity. The shear stress and shear rate on the funnel wall were calculated using the volume of the mud coming out at different points. It was found that both the plastic and apparent viscosities can be estimated using consistency plots.
In the work below, we will derive the equations that could be directly used for the determination of the rheological parameters in the oil field, for Newtonian and non-Newtonian fluids.

A model for fluid height (h) as a function of time (t) is developed and rheological properties are then determined from the best fit of the data to the model.
First, the mass balance for funnel can be given by: dV/dt = -Q(h) *(eq.69)*

With V = $\frac{\pi}{3}\left(\frac{R_F}{H_F}\right)^2 h^3$ *(eq.70)*

By substitution, we obtain the differential equation:

$\pi\left(\frac{R_F}{H_F}\right)^2 h^2 \frac{dh}{dt}$ = -Q(h) *(eq.71)*

The purpose is to determine rheological properties using the time elapsed and height of fluid displaced.
For Newtonian flow, the Hagen-Poiseuille equation can be substituted into the differential equation to give:

$$\pi\left(\frac{R_F}{H_F}\right)^2 \left(\frac{8\mu L}{\pi R^4}\right) \int_{h_0}^{h} \frac{h^2}{[\rho g(h+L)]}\, dh = -t \qquad (eq.72)$$

By integration, and using the total drainage time t_f, the viscosity of a Newtonian fluid can be given by:

$$\mu = \left[\frac{R^4}{8L}\left(\frac{H_F}{R_F}\right)^2\right]\left[\frac{\rho g}{Lh_0 - 1/2h_0^2}\right] t_f \qquad (eq.73)$$

For non-Newtonian fluids, several researchers have found equations that describe the apparent viscosity, plastic viscosity, and yield point.
For a simple calculation of the apparent viscosity, four equations were proposed and their results were compared to the viscosity obtained by a rotational viscometer. These equations only depend on Marsh funnel time or on the time and fluid density:

1- $\mu_a = \rho(t - 25)$ Introduced by Pitt *(eq.74)*

2- $\mu_a = \rho(t - 28)$ Modified from Pitt by Almahdawi et al. *(eq.75)*

3- $\mu_a = -0.0118t^2+1.6175t-32.168$ *(eq.76)*

4- $\mu_a = \exp\left[\frac{\ln(\frac{t-24.5}{0.58})}{1.2} + \ln(\rho)\right]$ *(eq.77)*

equation number 4 is expressed in the usual field conditions where the volume is in quart, the viscosity is in centipoise, the density is in g/cm^3, and 24.5 is the discharge time of the same volume of negligible viscosity. 0.58 and 1.2 are characteristic values of the funnel. A comparison between the values obtained from these equations with the laboratory values are given in the table below, for different fluids having different densities.

Marsh time (s)	density(g/cc)	visc. from lab	visc(eq. 4)	visc(eq. 1)	vis(eq. 2)	vis(eq. 3)
40.15	1.025	11.5	15.969666	15.52875	12.45375	13.75276
36.8	1.032	10	13.154589	12.1776	9.0816	11.37597
35.14	1.045	10	11.804411	10.5963	7.4613	10.10008
34.58	1.05	10.25	11.338347	10.059	6.909	9.654988
34	1.053	10.75	10.822844	9.477	6.318	9.1862
44.6	1.03	15	19.768662	20.188	17.098	16.50041
44.4	1.04	15	19.794942	20.176	17.056	16.38695
43.21	1.05	15	18.98428	19.1205	15.9705	15.69235
42.03	1.05	15.25	17.981154	17.8815	14.7315	14.97058
40.9	1.051	15.75	17.026129	16.7109	13.5579	14.24859
55	1.03	20.5	27.983182	30.9	27.81	21.0995
55.6	1.035	20	28.57924	31.671	28.566	21.28695
49.88	1.04	20.5	24.243	25.8752	22.7552	19.15433

49.13	1.047	21	23.803658	25.26411	22.12311	18.81744
49	1.049	21	23.744183	25.176	22.029	18.7577

Table 5: comparison between the apparent viscosities obtained experimentally and using the derived equations

The difference in the values is better shown in the graph below (figure 36):

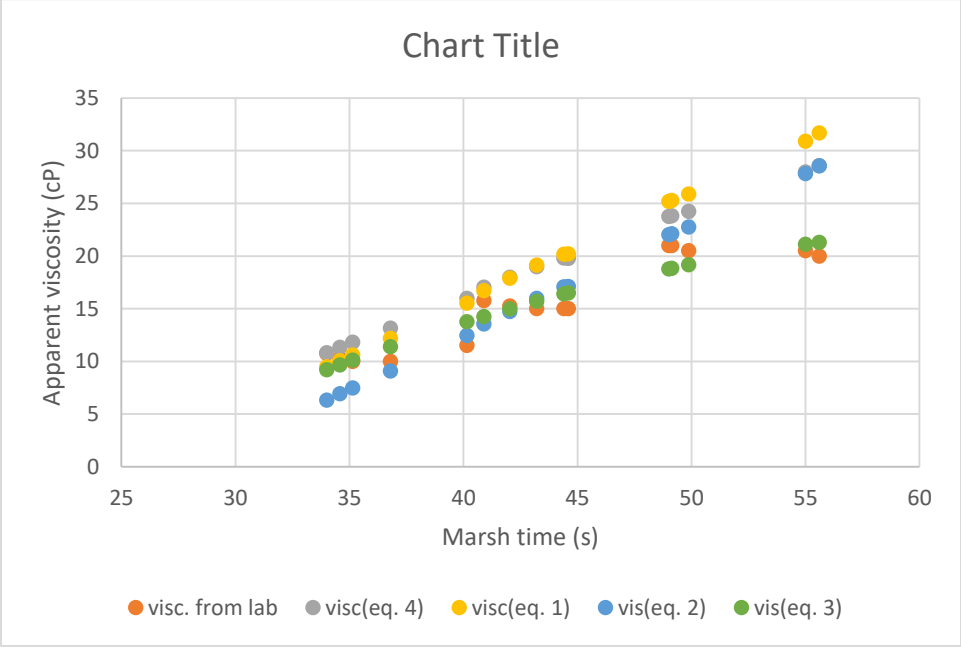

Fig. 36: comparison between the viscosities obtained from different equations

As it is shown, the relationships obtained from the Marsh time and the one modified from Pitt are more close to the values obtained from the rotational viscometer, and are recommended to use for simple and quick calculations of the slurry viscosity in the oil field.

For the determination of the plastic viscosity and the yield point, by using a Marsh funnel, the two parameters that should be calculated and continuously monitored in any CRI operation, the wall shear stress and wall shear rate of the funnel should be determined. The equations for the wall shear stress at the outlet are given by:

$$\tau_w = \begin{cases} \frac{1}{2}\rho g h(1-f^2)\frac{R_T}{H_T} & H_T + H_C \geq h > H_T \\ \frac{1}{2}\rho g(1-f^2)R_T & h \leq H_T \end{cases} \quad (eq.78)$$

With: R_T radius of copper tube (0.00238 m)
H_T height of copper tube (0.0508 m)
R_C radius of cone mesh (0.06985 m)
f is a dimensionless coefficient called the flow factor (rate factor). It is a function of the final discharge time T_F, and given by: $f=\frac{38}{T_F}$
for Newtonian fluids, the wall shear rate is given by:

$$-\dot{\gamma}_w = \frac{7\sqrt{2g}}{4R_T\sqrt{H_T}} fh = 14435.41fh \qquad (eq.79)$$

For non-Newtonian fluids, the shear rate is given by:

$$-\dot{\gamma}_w = \frac{7\sqrt{2g}}{4R_T H_T} fh^{\frac{1}{2}} = 64046.79fh^{\frac{1}{2}} \qquad (eq.80)$$

By calculation of the apparent viscosity and plastic viscosity as a function of the shear stress at a shear rate of 1020 and 510, and substituting them with the equations of shear rate equal to these values, we obtain the plastic viscosity and yield point for the non-Newtonian fluid [43,44,49]:

$$\eta = 0.0105493\rho(1-f^2)f^{-\frac{2}{3}} \qquad (eq.81)$$

$$and \quad \tau_0 = 3.7048 * 10^{-3}\rho(1-f^2)f^{-\frac{2}{3}} \qquad (eq.82)$$

ii. Rotational viscometer

This viscometer provides more meaningful measurement of the rheological characteristics of a slurry. The slurry is sheared at a constant rate between an inner bob and an outer rotating sleeve. Six standard speeds with a variable speed setting are available with the equipment. For most models designed foe field use, only two standard speed are possible. The dimensions of the bob and rotor are chosen so that the dial reading is equal to the apparent Newtonian viscosity in centipoise at a rotor speed of 300 rpm. At other rotor speed, the apparent viscosity will be given by:

$$\mu_a = \frac{300\theta_N}{N} \qquad (eq.83)$$

Where θ_N is the dial reading in degrees, and N is the rotor speed in revolution per minute.

This viscometer could also be used to determine the flow parameters of the Bingham plastic rheological model. This model is characterized by two parameters which are the plastic viscosity (expressed in centipoise), and yield point (expressed in lbf/100ft^2) of the fluid. The plastic viscosity will be computed as

$\eta = \theta_{600} - \theta_{300}$ *(eq.84)*

where θ_{600} is the dial reading while operating at 600 rpm, and θ_{300} is the dial reading at 300 rpm. The yield point is computed using:

$\tau_0 = \theta_{300} - \eta$ *(eq.85)*

Another rheological parameter could be determined using this instrument which is the gel strength, expressed in lbf/100ft^2. It is obtained by noting the maximum dial reflection when the rotational viscometer is turned at a low rotor speed (usually 3 rpm) after the mud has remained static for some period of time [36].

In this test, the viscometer cup is filled to the top of the dashed line and placed on the base of the rheometer. When the cup is positioned, the rheometer is turned onto its highest setting of 600 rpm. The degree dial should stabilize before taking the first reading. After that, subsequent measurements at 300, 200, 100, 6 and 3 rpm are recorded as well with the resulting dial reading. The data are then transformed to shear stress and shear rate, respectively

Fig. 37: Marsh-funnel (to the left) and rotational viscometer (to the right)

a) Rheological models

Rheological properties are manifestation of the rate and nature of the deformation that occurs when the fluid is stressed, they are one of several flow characteristics of a material. They should be determined to be able to predict the fluid behavior in a process, and to determine the energy requirement for fluid transportation.

Most slurries used in CRI are considered to be non-Newtonian fluids, especially plastic fluid and pseudoplastic fluid; having each different rheological properties. So the representation of different slurries in varying injection environments is difficult by only one rheological model. The Bingham fluid model and the power law fluid model are the two most common rheological models to represent fracturing fluids. These models are used for modelling non-Newtonian fluids, along with other models like Herschel-Bulkley model, Robertson-Stiff model and Casson model. Below are discussed the models applied on each type of

non-Newtonian fluid, and a discussion is made to know which model is the most suitable to use in case of slurry design in CRI operation.

a) Non Newtonian fluids

Non Newtonian fluids are fluids in which the relation between shear stress and shear rate is not linear; their flow properties are independent of the duration of shearing, and can be described by the equation:

$$\tau_{xy} = f(\dot{\gamma}_{xy}) \qquad (eq.86)$$

It implies that the shear, at any point within the sheared fluid, is determined solely by the current value of the shear stress at that point, or vice versa. They could be divided into four different types:

Fluids with properties time independent,

Fluids with properties time dependent,

Fluids with characteristics similar to solid bodies,

Complex fluids.

In our case, we will be working on the first category of non-Newtonian fluids, which properties are time independent.

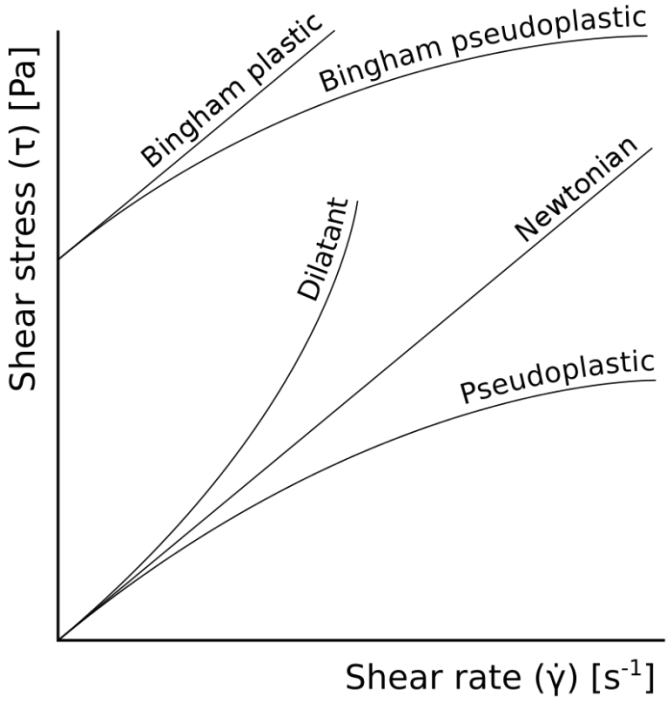

Fig. 38: Classification of fluids with shear stress as a function of shear rate

1- Fluids with time independent properties
   a) Pseudoplastic fluids

These types of fluids have an apparent viscosity: the ratio between shear stress and rate, that decreases with the increment of the shear rate. For most of the pseudoplastic fluids, the following limit variables could be introduced:

$$\lim_{\dot{\gamma}_{xy}\to 0} \frac{\tau_{xy}}{\dot{\gamma}_{xy}} = \eta_0 \quad \text{zero shear viscosity} \qquad \textit{(eq.87)}$$

$$\lim_{\dot{\gamma}_{xy}\to \infty} \frac{\tau_{xy}}{\dot{\gamma}_{xy}} = \eta_\infty \quad \text{infinite shear viscosity} \qquad \textit{(eq.88)}$$

Pseudoplastic fluids are characterized by a curve passing through the origin. A graph of apparent viscosity vs. shear rate in logarithmic scale (figure 39), shows that the central region of the curve is piecewise linear. This behavior is described by a power-law model:

$$\tau_{xy} = k(\dot{\gamma}_{xy})^n \qquad \textit{(eq.89)}$$

Where the two model parameters are n: the power-law index (shows how much the behavior of the fluid departs from a Newtonian fluid), and k: the fluid consistency coefficient; it indicates the degree of fluid viscosity. n=1 for Newtonian fluids, and n≠1 for non-Newtonian fluids. In particular, for pseudoplastic behavior n<1. The shear-thinning degree will be greater for lower values of the power-law index.

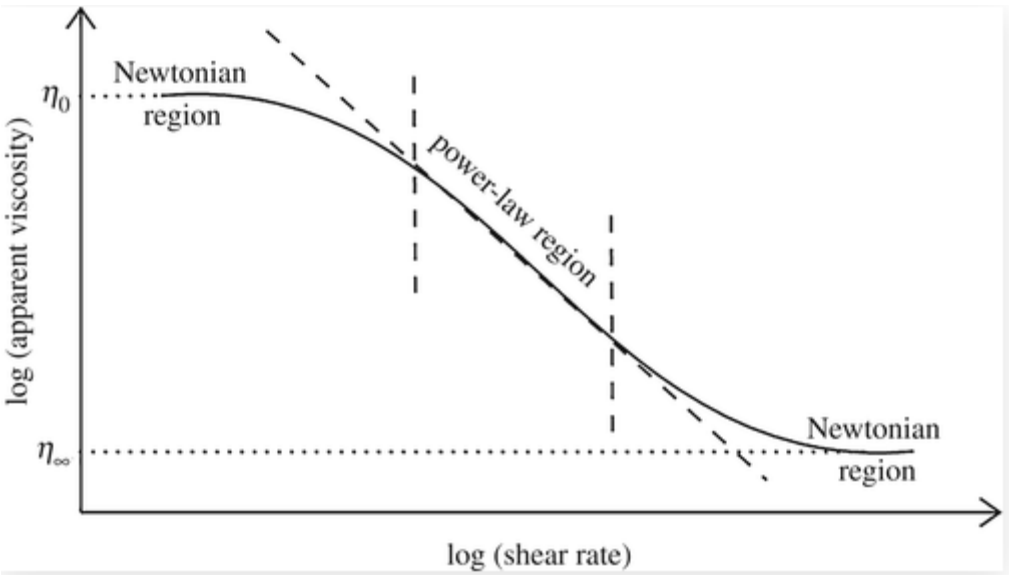

Fig. 39: Qualitative representation of the apparent viscosity behavior for a shear-thinning fluid

Dilatant or shear-thickening fluids:

These materials are similar to shear-thinning material as they show no yield stress; but with increasing shear rate, the apparent viscosity increases. For these fluids, the exponent is n>1. When a shear rate is applied to these fluids, the particles reorder to reduce the influence of the shear rate. By reordering, the overall shear force can be reduced. If a small shear rate is applied, the particles will have enough time to reorder. However, by applying a high shear rate, the particles do not have the required time to reorganize that will lead to the build-up of a significant shear force.

b) Bingham plastic fluids

In this class of material, a minimal yield stress τ_0 exists and should be exceeded before deformation (or flow) occurs. For stress levels greater than τ_0 the structure loosens and the material behaves as a viscous fluid. The Bingham plastic fluid has a linear flow curve for $|\tau_{xy}| > \tau_0$ and is characterized by a constant value of plastic viscosity.

The simplest and most widely used mathematical equation used to model this kind of flow behavior is written as:

$$\tau_{xy} = \tau_0^B + \eta\dot{\gamma}_{xy} \quad \text{if } \tau_{xy} > \tau_0^B \qquad \textit{(eq.90)}$$

$$and\ \dot{\gamma}_{xy} = 0 \quad \text{if } \tau_{xy} \leq \tau_0^B \qquad (eq.91)$$

τ_0^B is the Bingham yield stress, and η the plastic viscosity.

c) Yield pseudoplastic fluids

These fluids have a yield point and apparent viscosity which have no linear relationship with the shear rate, as observed for pseudoplatic fluids. The apparent viscosity in these fluids decreases with the increase of the shear rate; opposite rheological behavior to that of a yield dilatant fluid.

The theoretical model that represents in the best way these fluids behavior is known as Herschel-Bulkley model; it is written for a simple shear flow rate as [34,35]:

$$\tau_{xy} = \tau_0^H + k(\dot{\gamma}_{xy})^n \quad \text{if } \tau_{xy} > \tau_0^H \qquad (eq.92)$$

$$and\ \dot{\gamma}_{xy} = 0 \quad \text{if } \tau_{xy} \leq \tau_0^H \qquad (eq.93)$$

b) Discussion

The requirements of the slurry used for fracturing like low friction pressure in the pipe, high pressure drop in the fracture, cuttings suspending capability, made it almost impossible modelling the rheological properties of the slurry as a Newtonian fluid.

The fracture geometry depends weakly on the viscosity. For the PKN fracture geometry, the fracture length x_f is proportional to $\eta^{-1/5}$, whereas the width w_0 is proportional to $\eta^{1/5}$, and the pressure is proportional to $\eta^{1/4}$. However, the leak-off is strongly dependent on the viscosity as it is proportional to $1/\eta^{1/2}$. Settling also depends strongly on the viscosity: the Stokes settling velocity of a suspension with volume fraction φ scales as $u \sim \eta^{-1}(1-\varphi)^5$.

The CRI is designed to generate a large fracture width to place large amounts of cuttings per fracture area; this will require a high viscosity fluid during injection resulting in the fluid exhibiting low leak-off and resulting in long fracture closure time. The long settling time favors the cuttings settling, and leaves the top part of the fracture mostly empty and prone to closure. So a large viscosity is required while pumping and a small viscosity is required to favor leak-off after shut-in.

In modelling the slurry in CRI operations, mostly three models could be used, Newtonian model, Bingham model, and finally the power-law model. It all depend on the carrying fluid rheology. In case of Newtonian fluids, the carrying fluid is water and the slurry formed has a constant viscosity which will only change with the temperature and pressure; and the percentage of additives is relatively low. For the fracture propagation and fluid flow within it, it is typical to include simplification of the fracture geometry as a planar form, and treating the fluid as Newtonian, and assuming flow to be laminar, whose viscosity that depend on the cuttings content is calculated from an empirical formula. The slurry is usually represented as a fluid-solid mixture of prescribed rheology and density with differential settling enabled from the suspension. Also, it was assumed that the cuttings are distributed uniformly across the fracture aperture and that slip between the solid particles and the carrier fluid is only due to gravitational settling. The solid particles tend to migrate transversely away from the fracture walls and accumulate at the fracture center where the shear stress is the lowest, and flow velocity is the highest.

However, in the case of non-Newtonian fluids, in general, the Bingham fluid model and power law fluid model are the most common rheological models to represent the fracturing slurry. The Bingham model is more suitable for describing plastic fluid. The slurry represented by this model remains in a state of flocculation at low stresses, while flowing as a viscous fluid at high stress, and have a linear relationship between shear stress and shear rate at high stresses. The power law model is suitable for pseudoplastic fluid, that are driven to flow under tiny stresses, and its viscosity decreases under shear strain. Other models like Herschel-Bulkley model, Robertson-Stiff model, and Casson model could also be used for fluid rheology characterization. They may be more accurate to describe the slurry, but they are not capable of modeling other rheological properties of it, such as two-phase flow of a water-slurry mixture and the precipitation-dissolution process. Neither exist analytical solutions nor a commercial software that are capable of performing the parameter sensitivity analysis and safety evaluation.

Depending on the type of the carrying fluid, and which type of behavior does he show, the rheological study of the fracturing slurry is made. If the carrying fluid is water, with only small quantity of additives, mainly guar gum, the slurry will be treated as a Newtonian fluid; but now it is not the case as a wide variety of wastes is intended to be injected, so more additives should be used to form the most suitable slurry and meet the design requirements. As more additives are used, more will the fluid behavior diverge to that of a yield fluid. In that case, experiments

have shown that the behavior of the fracturing slurry made could be best described by the Bingham model or power law model to meet the design qualifications.
In all cases, the characterized slurry, when tested by a Marsh funnel, should have a funnel viscosity greater than 60 seconds/quart (between 60 and 90 s/quart), with a waste concentration ranging from 5 to 35% of solids by volume. The slurry should be characterized by its funnel viscosity (s), plastic viscosity (cP or Pa*s), and yield point (Pa); that in case of the Bingham model could be calculated as follows [48]:

$$\eta = 12.73*10^{-8}(2.84 - 456.4/T^2)*T*\rho \qquad \textit{(eq.94)}$$

$$\tau = 35420*\eta/T \qquad \textit{(eq.95)}$$

These equations are obtained from measurements done using a VBR-2 Funnel. And in case of the use of power law model, the apparent viscosity, consistency coefficient and flow index should be determined.

Also, another parameter should be observed during injection of the slurrified fluid, which is the pressure drop during injection (injection in annular space or tubing) which can be calculated based on both models: power law and Bingham model:

In case of power law fluid, we consider a CRI operation where the slurry density is 1260 kg/m^3, its apparent viscosity is 161 cP, the power law index is n= 0.26 and the slurry consistency coefficient is k=0.15. we consider an injection flow rate of 4 bbl/min (0.64 m^3/min). in case of tubing injection with an internal diameter of 4.27 in. (0.1084 m), and a total length of 2000 m [49]:

$$V=\frac{Q}{A} = \frac{0.64}{\frac{\pi}{4}(0.1084)^2} = 69.35 \text{ m/min} = 1.156 \text{ m/s} \qquad \textit{(eq.96)}$$

$$Re=\frac{\rho * v^{(2-n)} * ID^n}{k(2\frac{3n+1}{n})^{n-1}}; \qquad \textit{(eq.73)}$$

$$Re= \frac{1260*1.156^{2-0.26}*0.1084^{0.26}}{0.15(2\frac{3*0.26+1}{0.26})^{0.26-1}} = 42065.52 \text{ (turbulent flow)}$$

In this case a friction factor given by: $f=y(Re)^{-z}$ *(eq.98)* should be calculated, with:

$$y= \frac{\log(n)+3.93}{50} = \frac{\log(0.26)+3.93}{50} = 0.067, \text{ and} \qquad \textit{(eq.99)}$$

$$z=\frac{1.75-\log(n)}{7} = \frac{1.75-\log(0.26)}{7} = 0.333 \qquad \textit{(eq.100)}$$

$$f=0.067*(42065.52)^{-0.333} = 1.93*10^{-3}$$

the pressure drop is given by:

$\Delta P = f * \rho * \frac{v^2}{R} * L$ *(eq.101)*

$\Delta P = 1.93 * 10^{-3} * 1260 * \frac{1.156^2}{0.0542} * 2000 = 119915$ Pa $= 1.199$ bar

$\frac{\Delta P}{\Delta L} = \frac{1.199}{2000} = 0.0005995\ bar/m$ *(eq.102)*

In case of Bingham model, we consider a fluid having a plastic viscosity of 15 cP ($15*10^{-3}$ Pa.s), a yield point equal to 38 lbf/100 ft^2 (18.19 Pa), and a density of 1258.18 kg/m^3, the slurry is being injected at the same flow rate and in a tubing having the same dimensions as in the previous case.

First a dimensionless Bingham number is calculated by: $Bi = \frac{\tau_{0*ID}}{\eta * v} = \frac{18.19*0.1084}{15*10^{-3}*1.156} = 113.71$ *(eq. 103)*

A function f(Bi) is calculated as follows: $f(Bi) = \frac{24+Bi\left[1-\left(\frac{Bi}{Bi+8}\right)^3\right]}{24+Bi\left[4-\left(\frac{Bi}{Bi+8}\right)^3\right]}$ $(eq.104)$

f(Bi)=0.116

$$Re = \frac{\rho * v * ID}{\eta} f(Bi) = 1219.3 \quad (eq.105)$$

The friction factor is: $f = \frac{2}{3Re}\left\{24 + Bi\left[1 - \left(\frac{Bi}{Bi+8}\right)^3\right]\right\} = 0.02459$ $(eq.106)$

Finally, the pressure drop is:

$$\Delta P = f * \rho \frac{v^2}{R} L = 15.26\ bar \quad (eq.106)$$

$$\frac{\Delta P}{\Delta L} = \frac{15.26}{2000} = 0.00763\ bar/m$$

It can be seen that the pressure drop along the pipe is small in case of both methods, but it is smaller in case of the use of the slurry characterized by the power law model.

Pressure drop leads to less efficient injection operations because the injection pressure will decrease, so more time will be taken to initiate a fracture, and also to propagate it; this could lead to the bridging of particles near the wellbore.

Among all the slurry components, the cuttings are found to be the most important ones on which studies should be made: first their concentration is one of the key parameters used to control fracture growth due to the change of gravity and slurry viscosity. In addition, settling of cuttings could lead to a blockage in both the well and the formation causing a risk to the injection operation. Also, the size of the solid particle was found to be a key factor in influencing underground storage capacity.

Knowing which additives are used to create the slurry is related to the type of the formation in which the injection will take place, and maintaining a minimum concentration of the mud residual on the cuttings is a key point in the slurry design. Oil, iron sulfides, asphaltenes, clays, … could all be present on the cuttings because their separation is quite difficult and costly; so the slurry should be designed in a way that is not affected by these residuals. In some cases, materials that create noise (detonation) could be added to the slurry during injection or shut-in to be able to detect the propagation of the main fracture or creation of branches or fissures while using the microseismic method because it has a limited ability in differentiating downhole seismic events from different sources. Also addition of radioactive tracers along with the use of logging program aids in the determination of the disposal domain.
In addition, the slurry composition and rheology has a great effect on the fracturing process and well injectivity; it controls the particle settlement velocity which affects the cuttings settlement inside the fracture and its closure.
A simulation was made on several wells in which several injection episodes have taken place. From the collected data, it was shown that the slurry components percentages have an effect on injectivity as shown (figure 40). Injectivity is equal to the average pumping rate divided by the net pressure (average inj. Pressure-virgin reservoir pressure). It gives an indication of how well the formation is accepting fluid during an injection episode.

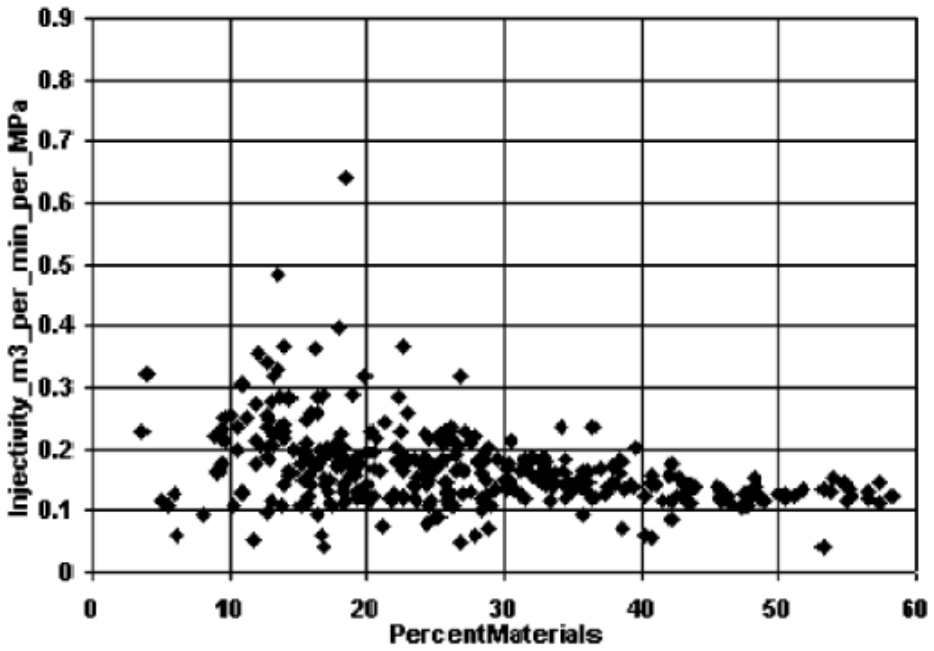

Fig. 40: Injectivity vs. percent materials

Slurry with high percentage of waste is expected to be more difficult to inject. On the figure above, it appears to be an envelope which causes slurries with high percent of waste to cause lower injectivity. The injectivity is higher when the percentage ranges between 10 and 30%.

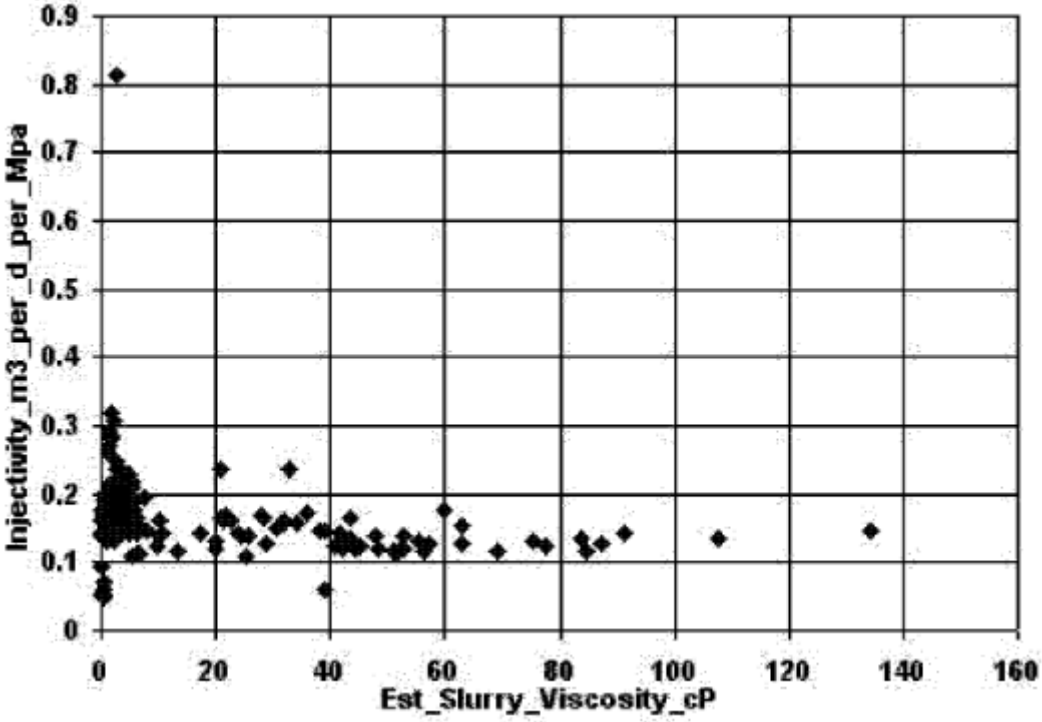

Fig. 41: Injectivity vs. slurry viscosity

Figure 41 shows how the injectivity is affected by the slurry viscosity. High viscosity slurry result in low injectivity as it is more difficult to inject in the formation, on the contrary for low viscosities. It could be noted that for viscosities higher than 40 cP, the injectivity values remain relatively constant; the viscosity no more has the capacity to reduce it [41].

V. Conclusion

CRI provides a secure operation by injecting cuttings and associated fluids up to several thousand meters below the surface into hydraulically created fractures. It is a method for managing drilling wastes with reduced cost, and reduction of their carbon footprints. Experience has proved that CRI operation is an environmentally safe and economically sound solution for exploration and production waste management, if the job is engineered and executed correctly with a well-defined monitoring program. The key is continuous monitoring to demonstrate containment and environmental security, to optimize the process and allow the reservoir state to be carefully tracked during the process. Simulations are performed for the anticipated downhole waste domain in order to guarantee containment within the selected underground formation, and perform sufficient design of surface facilities.

Fracture simulation was done by using the PKN model to predict the fracture length and width, by assuming a constant height. More advanced methods could be used for the fracture geometry determination, for example the pseudo 3D model, which does not require estimating the fracture height, but requires input of the magnitude of minimum horizontal stress in the zone to be fractured and in the zones immediately above and below. But this model is costlier.

Pressure response simulation and analysis of reservoir condition, along with offset data, deformation analysis, and microseismic data (if available). Lack of proper pressure analysis after each injection batch raises the risks of formation damage and may lead to permanently plugged wells. Also, correct flow rate and injection pressure are necessary to laterally propagate solids farther away from the wellbore and into the formation fir a successful CRI operation. Preexisting fractures, joints, and faults can redirect or modify the propagation direction of the induced fractures

Rheological modelling of the slurry in every cuttings re-injection operation is a key point in preventing many inconveniences that could occur while injecting, like particle settling while injecting that could lead to line blockage, and gradually to the loss of the well for additional injection, also, it could lead to the loss of the well injectivity. The rheological design remains one of the biggest challenges or technology gaps in CRI operations.

Bingham model and power law model are the two common models used to describe the slurry rheology and its rheological parameters (apparent viscosity,

plastic viscosity, and yield points) were derived using several equations. Also, the pressure drop inside the injection tubing was calculated in case of both models. The damage of the formation while performing a CRI is inevitable, that is why field operators must change the injection strategy, pressure, rate, and slurry properties in order to extend the well life, and delay or avoid the filter cake formation.

Future progress is necessary to understand better the disposal domain characterizations during the planning and execution phase, including the use of 3D simulators and real-time monitoring of injection parameters and improved disposal domain models and fracture network. In addition, to maximize the volume of slurry waste disposal in the safest and economically most efficient matter, continuous monitoring of all parameters and real-time visualization of disposal domain is recommended.

References:

1. Overview of Environmental Management by Drill Cuttings Re-Injection Through Hydraulic Fracturing in Upstream Oil and Gas Industry. Mansour Zoveidavianpoor, Ariffin Samsuri and Seyed Reza Shadizadeh. Chapter 17. 2011.

2. https://www.slb.com/videos/cuttings-reinjection-service

3. Fluids Environmental Services. Effective, environmental waste management solutions. Baker Hughes

4. Johannes Karl Fink, in Petroleum Engineer's Guide to Oil Field Chemicals and Fluids, 2012

5. M. Ibrahim Khan, M.R. Islam, in The Petroleum Engineering Handbook: Sustainable Operations, 2007

6. Cuttings re-injection must match increased drilling efficiency. New technology assisting in downhole disposal. Offshore journal. September 1 2000.

7.An introduction to slurry injection technology for disposal of drilling wastes, pdf

8. Deep Underground Injection of Waste from Drilling Activities, Faculty of Mining, Geology and Petroleum Engineering, University of Zagreb, 10000 Zagreb, Croatia. Published: 27 March 2020. Pdf

9. Challenges for monitoring and verification of drill cuttings reinjection performance. Ahmed s. Abou-Sayed, Quanxin Guo, Gary Wang, John D. McLennan and Karim Zaki, Advantek International, Houston Texas, USA. SPE/ISRM

10.Practical Rock Engineering-Chapter 10-In Situ and Induced Stresses

11.https://people.eng.unimelb.edu.au/stsy/geomechanics_text/Ch3_Strs_Ground.pdf

12. Drill Cuttings Disposal- An Overview of the five Most Common Methods. The panther companies. October 8 2020.

13.Field Experiences with Oilfield Waste Disposal Through Slurry Fracture Injection. Margaret Srinivasan, Micheal S. Bruno, Roman A. Bilak. June 1997.

14. Structural Mechanics, Fluid-Structure Interaction, Poroelasticity. Multiphysics Encyclopedia. Published October 31, 2014

15. Panos Papanastasiou, Ernestos Sarris, in Porous Rock Fracture Mechanics, 6.2.2 Rock deformation. 2017

16.ClASS I FRACTURE SLURRY INJECTION, A summary of the Technology and Recommendation for Implementation, by Joe Kordzi, February 26, 1998

17. Finnie’s Notes on Fracture Mechanics- C.K.H. Dharan et al. (Springer, 2016) (Chapter 3)

18. Mechanical properties of thermosets, Fracture mechanics: linear elastic fracture mechanics. M.J. Mullins, D.Liu, H.J.Sue , in Thermosetes, 2012.

19. Applied Petroleum Geomechanics, Jon Jincai Zhang, 2019
In situ stress regimes with lithology-dependent and depletion effects,
5.1 In situ stresses in various faulting regimes.

20. http://home.agh.edu.pl/~cala/hoek/Chapter10.pdf

21. Hydraulic Fracturing in Unconventional Reservoirs, Hoss Belyadi, Fatemeh Belyadi, 2nd edition, 2019. Numerical simulation of hydraulic fracturing propagation.

22. Elements of Hydraulic Fracturing. Richard Nolan-Hoeksema. Oilfield Review, 2006

23. Handbook of Hydraulic Fracturing, John Wiley & sons, Inc.; 2016. Chapter 5, Hydraulic fracturing

24. Feasibility Study of Drill Cuttings Re-Injection in the Ahwaz Field Iran. Saeed Majidaie and Seyyed R. Shadizadeh, SPE, Petroleum University of Technology (PUT). 4-6 August 2009.

25. A step towards to Minimize Environmental Footprint: An Innovative System to Dispose Generated Cement Waste on a Zero Discharge Artificial Islands. Rudra Pratap Singh, Khalid Al-Wahedi, Rashid Al Kindi, Bassam G Elatreche, Maurizio Cesetti, Jose Alzate, Mhammed Benygzer, Mohammed Haddad and Mahmoud Hassan, ADMA – OPCO; Cliff Kirby, Phalgun Paila, and Ala Suleiman Baker Hughes, a GE company; Alexey Ruzhnikov, Schlumberger. SPE-188477-MS. 13-16 November 2017.

26. https://www.malvernpanalytical.com/en/products/technology/light-scattering/laser-diffraction

https://www.atascientific.com.au/measurement-analysis-particles/

27. Hydraulic Fracturing, Unlocking America's Natural Gas Resources. America's Oil and Natural Gas Industry. August 2017.

28.Mewis, Jan; Wagner, Norman J. (2012). Colloidal Suspension Rheology. Cambridge university, p19.

29. Streeter, Victor Lyle; Wylie, E. Benjamin; Bedford Keith W. (1998). Fluid Mechanics.

30. Incropera, Frank P.; et al. (2007). Fundamentals of Heat and Mass Transfer. Wiley.

31. IPropagation, proppant transport and the evolution of transport properties of hydraulic fractures, Published online by Cambridge University Press: 19 September 2018. Jiehao Wang, Derek Elsworth and Martin K. Dension.

32. Fracturing Fluid Components, Carl Montgomery, Published: May 17th 2013

33. Mathematical modelling with experimental validation of viscoelastic properties in non-Newtonian fluids. C. M. lonescu, I. R. Birs, D. Copot, C. I. Muresan and R. Caponetto. Published 11 May 2020.

34. Microfluids: Modelling, Mechanics and Mathematics, Bastian E. Rapp, 2017. Chapter 9: Fluids

35. APPLIED DRILLING ENGINEERING, CHAPTER 2: Drilling fluids.

36. Challenges for monitoring and Verifications of Drill Cuttings Reinjection Performance. Abou-Sayed, A.S., Guo, Q., Wang, G., McLennan, J.D., and Zaki, K. 20-23 October 2002.

37. Fractured Water-Injection Wells: A Pressure Falloff Test for Determining Fracture Dimensions. Koning, E.J.L., and Niko, H. 22-25 September.

38. Pressure Transient Analysis in Fractured Produced Water Injection Wells. Van Den Hock, P.J., 8-10 October 2002008, Gulf Publishing Company) - libgen.lc.pdf

39. Deep Underground Injection of Waste from Drilling Activities. Nediljka Gaurina-Medimurec, Borivoje Pasic, Petar Mijic and Igor Medved. 27 March 2020.

40. DEVELOPMENT OF IMPROVED OIL FIELD WASTE INJECTION DISPOSAL TECHNIQUES. Terralog Technologies USA, Inc. Arcadia, California. November 2002.

41. Apparent Viscosity Direct from Marsh Funnel Test. Faleh H. Almahdawi, Ahmed Zarzor Al-Yaseri and Nagham Jasim. March 2014

42. Lancelotta, 2009. Geotechnical Engineering, 2nd edition, Taylor and Francis, New York.

43. Newly Developed Correlations to Predict the Rheological Parameteres of High-Bentonite Drilling Fluid Using Neural Networks. Gowida, Ahmed; Elkatatny, Salaheldin; Abdelgawad, Khaled; Gajbhiye, Rahul. 2020

44. The Marsh Funnel and Drilling Fluid Viscosity: A New Equation for Field Use. Pitt, M.J. (2000).

45. Rheological Characterization of Hydraulic Fracturing Slurries. Shah, S.N. 1993

46. Reologia ed idraulica dei fluidi di perforazione, Roberto Maglione, Raffaele Romagnoli

47. Measurement of the Plastic Viscosity and Yield Point of drilling fluids. D. N. Delikesheva, A.Kh. Syzdykov, J.A. Ismailova, A.A. Kabdushev, G.A. Bukayeva. 2020.

48. Investigation of Drill Cuttings Reinjection Environmental Management in Iranian Ahwaz Oilfield, S. R. Shadizadeh, S. Majidaie, M. Zoveidavianpoor, 2011

49. Rheological analysis of Newtonian and non-Newtonian fluids using Marsh funnel: Experimental study and computational fluid dynamics modeling. Zhaochuan Li, Lihui Zheng, Weian Huang. 20 January 2020

50. More Companies and US States Eyeing Slurry-Injection Technology. Brian Balboa. Journal of Petroleum Technology, October 20,2020